AD-A044 034 RAYTHEON CO WALTHAM MASS RESEARCH DIV F/G 9/5
COST-EFFECTIVE GAAS READ IMPACT TRANSMITTERS.(U)
MAY 77 R N WALLACE F30602-76-0143
UNCLASSIFIED S-2166 RADC-TR-77-178 NL

1 OF 2
AD A044034

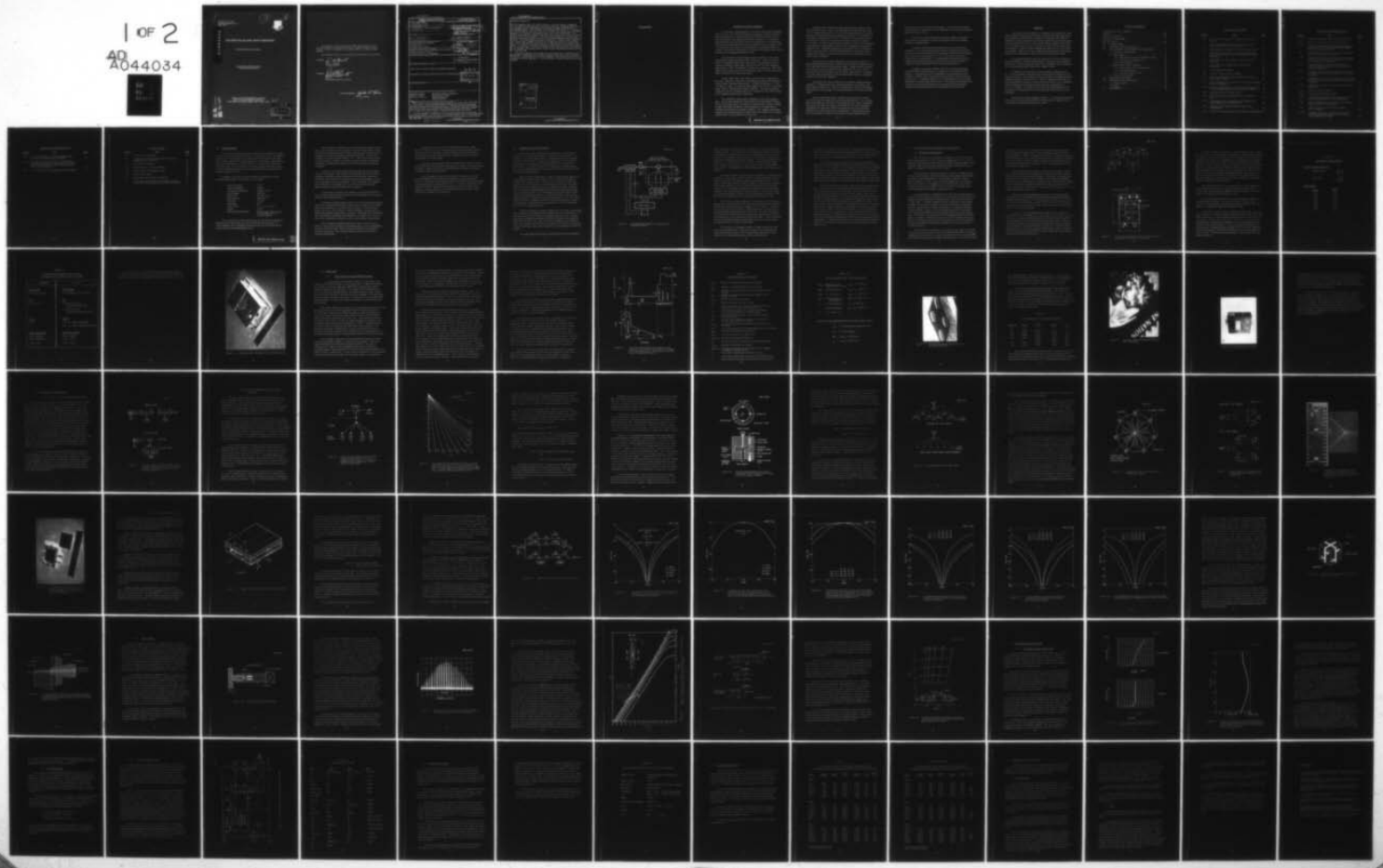

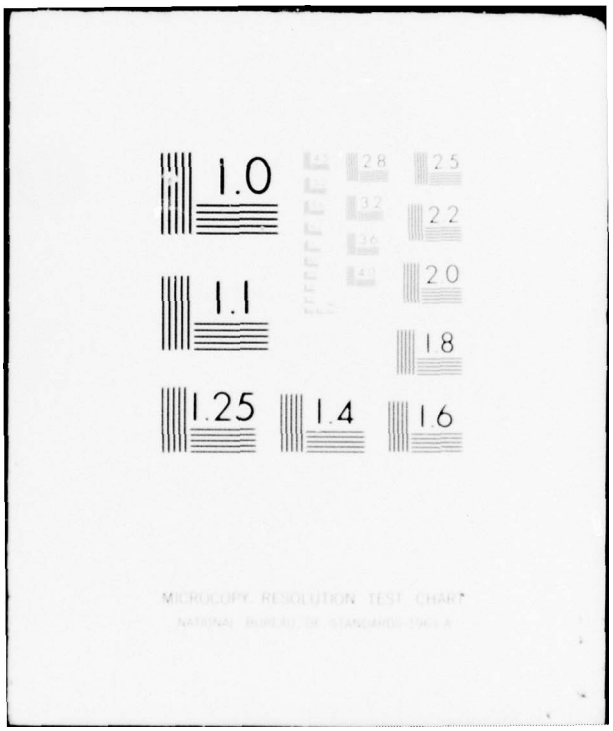
1.0
1.1
1.25
1.4
1.6
2.8
2.5
3.2
2.2
3.6
2.0
4.0
1.8
MICROCOPY RESOLUTION TEST CHART
NATIONAL BUREAU OF STANDARDS-1963-A

RADC-TR-77-178
Scientific Report No. 1
May 1977

AD A044034

COST-EFFECTIVE GaAs READ IMPATT TRANSMITTERS

Raytheon Research Division

Approved for public release;
distribution unlimited

ROME AIR DEVELOPMENT CENTER
AIR FORCE SYSTEMS COMMAND
GRIFFISS AIR FORCE BASE, NEW YORK 13441

AD No.
DDC FILE COPY

DDC
RECEIVED
SEP 13 1977
B

This report has been reviewed by the RADC Information Office (OI) and is releasable to the National Technical Information Service (NTIS). At NTIS it will be releasable to the general public, including foreign nations.

This technical report has been reviewed and approved for publication.

APPROVED: S. A. Roosild

SVEN A. ROOSILD
Project Engineer

APPROVED: Robert M. Barrett

ROBERT M. BARRETT
Director
Solid State Sciences Division

FOR THE COMMANDER: John P. Huss

Plans Office

Unclassified

SECURITY CLASSIFICATION OF THIS PAGE (When Data Entered)

REPORT DOCUMENTATION PAGE	READ INSTRUCTIONS BEFORE COMPLETING FORM
1. REPORT NUMBER (19) (18) RADC-TR-77-178	2. GOVT ACCESSION NO. / 3. RECIPIENT'S CATALOG NUMBER
4. TITLE (and Subtitle) (6) Cost-Effective GaAs Read IMPATT Transmitters,	5. TYPE OF REPORT & PERIOD COVERED (9) Scientific Report No. 1, 29 MAR-3/29/76 - 9/29/76 29 Sep 76,
	6. PERFORMING ORG. REPORT NUMBER (14) S-2166
7. AUTHOR(s) (10) R. N. Wallace	8. CONTRACT OR GRANT NUMBER(s) (15) F30602-76-0143
9. PERFORMING ORGANIZATION NAME AND ADDRESS Raytheon Research Division 28 Seyon Street Waltham, MA 02154	10. PROGRAM ELEMENT, PROJECT, TASK AREA & WORK UNIT NUMBERS (16) 62702F 46001803 (17) 18
11. CONTROLLING OFFICE NAME AND ADDRESS Deputy for Electronic Technology (RADC/ETSD) Hanscom AFB, MA 01731 Contract Monitor: Sven Roosild	12. REPORT DATE (11) May 1977
	13. NUMBER OF PAGES ~~94~~ (12) 97 p.
14. MONITORING AGENCY NAME & ADDRESS (if different from Controlling Office)	15. SECURITY CLASS. (of this report) Unclassified
	15a. DECLASSIFICATION/DOWNGRADING SCHEDULE N/A

16. DISTRIBUTION STATEMENT (of this Report)

Approved for public release; distribution unlimited.

DDC RECEIVED SEP 13 1977 B

17. DISTRIBUTION STATEMENT (of the abstract entered in Block 20, if different from Report)

18. SUPPLEMENTARY NOTES

19. KEY WORDS (Continue on reverse side if necessary and identify by block number)

Gallium Arsenide
IMPATT Diodes
Microwave Devices
Microwave Power Combiners
Microstrip Circuits
Epitaxial Material
Semiconductors

20. ABSTRACT (Continue on reverse side if necessary and identify by block number)

The objective of this program is to develop a low-cost 5-GHz 40-W FM CW transmitter, using GaAs Read IMPATT diodes as RF power-generating elements, suitable for data-link applications. Results of work so far indicate that the RF performance goals for the transmitter can be achieved, but that size, weight, and primary power consumption goals will be exceeded.

We have designed a transmitter system that separates the unit into four main subassemblies: a VCO-driver, a multidiode output stage, a multichannel →

DD FORM 1 JAN 73 1473 EDITION OF 1 NOV 65 IS OBSOLETE

298320

Unclassified

SECURITY CLASSIFICATION OF THIS PAGE (When Data Entered)

ABSTRACT (Cont'd.)

current regulator, and a DC-to-DC inverter. The VCO-driver, producing 3.3-W output at 5 GHz, has been assembled and tested. Epitaxial wafers for the high-power GaAs Read diodes to be used in the output stage have been successfully grown. The best diode result obtained so far is 21-W CW output at 4.86 GHz with 29.5 percent efficiency, and five of six wafers processed have produced 15-W diodes. The diodes permit a four-diode output stage. Six monthly shipments of six diodes representative of those to be used in the output stage have been made to RADC. The output stage design uses a nonresonant parallel-type power combiner based on the modified Wilkinson hybrid described by Gysel. Four single-diode oscillator modules are coupled to this combiner. The combiner and modules are realized in trapped inverted microstrip (TIM) line. Basic TIM-line test circuits have been assembled and are awaiting evaluation. A resonant-cavity power combiner design is also available for possible use as an output stage. The circuit design for the multichannel current regulator is complete. A commercial DC-to-DC inverter has been selected for use in the transmitter.

Tasks which remain to be completed include fabrication of additional high-power diodes, fabrication of the diode modules and four-port power combiner in TIM line, construction of the current regulator, and assembly and test of the complete transmitter package. A cost-performance tradeoff analysis must also be made.

ACCESSION for
NTIS White Section ☑
DDC Buff Section ☐
UNANNOUNCED ☐
JUSTIFICATION
BY
DISTRIBUTION/AVAILABILITY CODES
Dist. and/or SPECIAL
A

EVALUATION

TECHNICAL REPORT SUMMARY

The objective of this program is to develop a deliverable breadboard model of a low-cost 5-GHz FM transmitter having 40-W output suitable for data-link applications. Gallium arsenide Read IMPATT diodes are to be used as RF power-generating elements in the transmitter. Preliminary analysis and the first six month's work on the program have indicated that the major RF performance goals for the transmitter can be achieved. However, goals for size, weight, and primary power consumption will be exceeded. The purpose of this report is to describe the program effort for the period 29 March through 29 September 1976.

The transmitter system design has been completed. Four major subassemblies make up the deliverable transmitter. These are the VCO-driver, the multiple-diode power output stage, the multichannel current regulator feeding the output stage, and the DC-to-DC inverter supplying high voltage (~130 V) to all IMPATT diodes in the transmitter. The transmitter operates from a 28-VDC primary power source and uses GaAs Read IMPATT diodes for RF power generation.

Design, fabrication, and testing of the VCO-driver subassembly have been completed. This unit is essentially a low-power FM transmitter which accepts a baseband input (70 KHz - 10 MHz) and produces ~3.3-W CW output at 5 GHz. It is electronically tunable over the 4.97-to-5.03-GHz range, and has 10-MHz peak deviation capability. This unit is awaiting integration with the remaining parts of the transmitter, after which testing of the complete system will be undertaken.

The transmitter output stage development is the major program task. This includes production of high-power GaAs Read IMPATT diodes for use in the output stage, development of single-diode oscillator modules in which the diodes can operate, and development of a suitable power-combining network for the oscillator modules. The complete output stage operates as an injection-locked oscillator and must combine four oscillator modules with a circuit efficiency of 70 percent.

PRECEDING PAGE BLANK-NOT FILMED

Epitaxial material growth and diode fabrication procedures, which can repeatably produce 5-GHz GaAs Read IMPATT diodes with more than 15-W CW output and 25 percent DC-to-RF conversion efficiency, have been demonstrated during the first six months of the program. The best diode performance obtained so far is 21-W CW output at 4.86 GHz with 29.5 percent efficiency, and five of six epitaxial wafers processed have yielded 15-W diodes. Six diodes representative of those to be used in the transmitter output stage have been shipped to RADC at the conclusion of each month's program effort. Additional epitaxial material must be grown so that more diodes can be fabricated. These diodes will form an inventory for use in meeting future delivery requirements (six diodes per month) and for use in output stage development.

The general form of the output stage circuit has been selected. A nonresonant parallel-type power combiner using a modified Wilkinson hybrid of the type described by Gysel has been chosen. Analysis has been carried out to define the loss and isolation levels required in the circuit, and to show that the selected combiner can meet these requirements. An alternative output stage design using a dielectrically-loaded resonant cavity power combiner has also been completed.

Preliminary RF circuit design for the oscillator modules has been completed. Measurements of the terminal impedance of the diodes under large-signal conditions are required to complete some details of the design. Following bias circuit design, the oscillator modules can be fabricated and tested.

Both the nonresonant power combiner and the oscillator modules are to be realized in trapped inverted microstrip (TIM) line. This medium offers advantages over the other transmission lines (microstrip, suspended microstrip, and balanced stripline) considered for use in the transmitter. Components for some basic TIM-line sections and for a two-port Gysel hybrid have been fabricated and are awaiting test. Following these tests the four-port power combiner will be fabricated and integrated with the

diode modules to form the power output stage. The resonant cavity power-combiner design is being held for use if difficulties arise with the previously untried TIM-line circuits.

Circuit design for the multichannel current regulator is complete. This unit must be assembled, tested, and integrated with the remaining transmitter subassemblies.

A standard commercially available inverter is to be used in the transmitter. One suitable unit has been selected, and based on the use of this unit, total current demand of the transmitter from the 28-V DC primary power source has been projected at ~15 A. The inverter is still to be ordered from the manufacturer. The possibility of reducing the size and weight and increasing the efficiency of the present inverter is being investigated through consultation with the inverter manufacturer.

In addition to assembly and final test of the transmitter package, several analytical tasks must also be completed in the remainder of the program. Reliability data on the components in the transmitter must be reviewed to confirm that the operating life and shelf life requirements can indeed be met. A complete analysis of cost and possible cost-size-weight-performance tradeoffs must also be made. The deliverable transmitter will obviously not represent the highest level of design refinement possible. Prospects for future improvement in performance will be surveyed.

PREFACE

The objective of this program is to develop a low-cost FM CW transmitter capable of producing 40-W output at 5 GHz for data-link applications. The transmitter is to use GaAs Read IMPATT diodes as active elements. Results of the work completed so far indicate that the RF performance goals of the transmitter can be met. In particular, diodes capable of more than 15-W CW output with more than 25 percent efficiency have been fabricated, and designs for compact circuits combining the outputs of four such devices are available. However, the size, weight, and primary power consumption objectives for the transmitter will be exceeded by the present design.

The program work has been carried out by the Research Division of Raytheon Company, Waltham, Massachusetts. The work was sponsored by the Air Force Systems Command, Rome Air Development Center, Hanscom AFB, Massachusetts under Contract No. F30602-76-0143.

At Raytheon, the work was carried out under the supervision of R. W. Bierig, Manager of the Microwave Semiconductor Laboratory at the Research Division. The growth and characterization of the gallium arsenide epitaxial wafers were directed by S. R. Steele. Design and fabrication of GaAs Read IMPATT diodes were under the direction of Dr. M.G. Adlerstein. Diode evaluation and circuit development were the responsibility of Dr. R. N. Wallace. Development of the VCO-driver subassembly in the transmitter was subcontracted to the Raytheon Special Microwave Devices Operation.

The Air Force Project Engineer was Mr. S. A. Roosild, RADC/ETSD. This report covered the period 29 March 1976 through 29 September 1976. The Raytheon internal report number is S-2166.

TABLE OF CONTENTS

LIST OF ILLUSTRATIONS

LIST OF ILLUSTRATIONS (Cont'd.)

LIST OF ILLUSTRATIONS (Cont'd.)

LIST OF TABLES

1.0 INTRODUCTION

This interim report describes the technical effort toward the development of a deliverable breadboard model of a cost-effective GaAs Read IMPATT transmitter. The transmitter is to produce 40-W CW output at 5 GHz with FM capability suitable for data-link applications. High-power, high-efficiency GaAs Read IMPATT diodes are being used as active elements in the power-generating stages of the transmitter. The work reported herein was carried out at the Raytheon Company Research Division during the period 29 March through 29 September 1976.

A number of specific performance goals were initially set for the breadboard transmitter. These goals are listed below.

Center Frequency	5 GHz
Tunable Bandwidth	60 MHz
Instantaneous Bandwidth	10 MHz (-1 dB)
Power Output	40 W CW
Input Power	28 V DC, 10 A
Operating Life	5000 hours
Shelf Life	7 years
Modulation	FM
Form Factor	$6.4 \times 1.7 \times 3.6$ in.^{3}
Weight	3.5 lb.
Noise (Total AM and FM)	30 dB or more below carrier level 100 MHz from the carrier frequency

To be complete, the noise specification must include the bandwidth in which the noise is measured. We have assumed that the total noise in a 1-kHz bandwidth that is 100 MHz removed from the carrier must be 30 dB or more below the transmitted power level.

PRECEDING PAGE BLANK-NOT FILMED

The instantaneous bandwidth and modulation specifications were also open to interpretation. Our interpretation was that the transmitter should be capable of FM operation with 10-MHz (maximum) peak-to-peak frequency deviation, and 10-MHz (maximum) modulating frequency. Power output variation at maxium deviation should be +0, -1 dB across the full electronically tuned range. Further, it should be possible to obtain a modulation sensitivity for 10-MHz input within 1 dB of the low-frequency modulation sensitivity.

A number of additional requirements were placed on the technical effort for the program. The design of the transmitter was to be such that quantities of 500 units could be manufactured for less than $2000 each. Constraints and tradeoffs in the design, fabrication and operation, and cost of the transmitter were to be identified. At the conclusion of the program, final testing of the transmitter was to be carried out by the Research Division and witnessed by the RADC project engineer.

At the end of each month of the program, six GaAs Read IMPATT devices representative of those being used in the transmitter were delivered to Rome Air Development Center.

Preliminary analysis indicated that most of the major RF performance goals for the breadboard transmitter could be met, and the first six months' work on the program has not changed this conclusion. Achievable goals include those for center frequency, tunable bandwidth, instantaneous bandwidth, FM capability, output power, and noise. Reliability of the high-power GaAs Read diodes is still under investigation, but it appears that these devices can be sufficiently reliable to meet the requirements of the program.

The breadboard transmitter will operate from a 28-VDC source. However, the current required by the present design is ~15 A, substantially in excess of the 10-A goal. There are some prospects for reducing the current requirements, either through efficiency improvements or by a tradeoff of output power.

Principally because of the size and weight of the power supply (DC-to-DC inverter), the size and weight goals for the transmitter package will be exceeded. Eventually, it will be possible to fit the RF portion of the transmitter into the specified volume, although the first breadboard will probably exceed this limit.

A precise cost projection for the transmitter must await the results of the final design choices, which still remain to be made. This cost analysis, as well as a study of possible cost and performance tradeoffs, will appear in the final report for the program.

In the remaining sections of this report, we first give an overall system description of the deliverable transmitter as presently planned (Sec. 2). The details of development work on each of the major subassemblies in the transmitter are then presented in Sec. 3. Section 4 summarizes the hardware deliveries which were made during the first six months of the program. Section 5 provides an overall review of the work and presents plans for the remainder of the program.

2.0 TRANSMITTER SYSTEM DESIGN

Figure 2-1 shows a functional block diagram for the deliverable transmitter as it is presently planned. Four major subassemblies – the VCO-driver, the power output stage, the multichannel current regulator, and the DC-to-DC inverter – make up the complete unit. The details of progress on the development of each subassembly are described in Sec. 3 of this report. The system design for the transmitter is essentially the same as that originally proposed, but there have been some changes within the individual subassemblies.

The VCO-driver subassembly accepts a baseband input signal in the range 70 KHz to 10 MHz and provides 3.3-W CW (typical) of frequency-modulated RF output at 5 GHz. The full 4.97-to-5.03-GHz tuning range specified for the transmitter is covered by electronic tuning. The power output of this driver should be more than sufficient to provide 10 MHz of electronic tuning (locking bandwidth) in the subsequent power output stage. The subassembly includes in a single package a low-power (100-150 mW) voltage-controlled Gunn oscillator, two injection-locked oscillator stages using GaAs IMPATT diodes to increase the output power to ~3.3 W, and the voltage and current regulators required for the Gunn and IMPATT stages. The total power consumption of the subassembly is ~61 W, substantially above the 33 W originally budgeted.

Design, fabrication, and initial testing of the VCO-driver subassembly were carried out by the Raytheon Special Microwave Devices Operation. The unit was delivered to the Research Division in September 1976. Original specifications called for operation of the IMPATT stage current regulators in the unit from 120-V DC. Since the inverter output has been changed to 130 V, for reasons to be described, the additional 10 V must be accomodated either by inserting a zener diode as shown or by readjusting the current regulators.

The output stage will consist of four high-power GaAs Read IMPATT

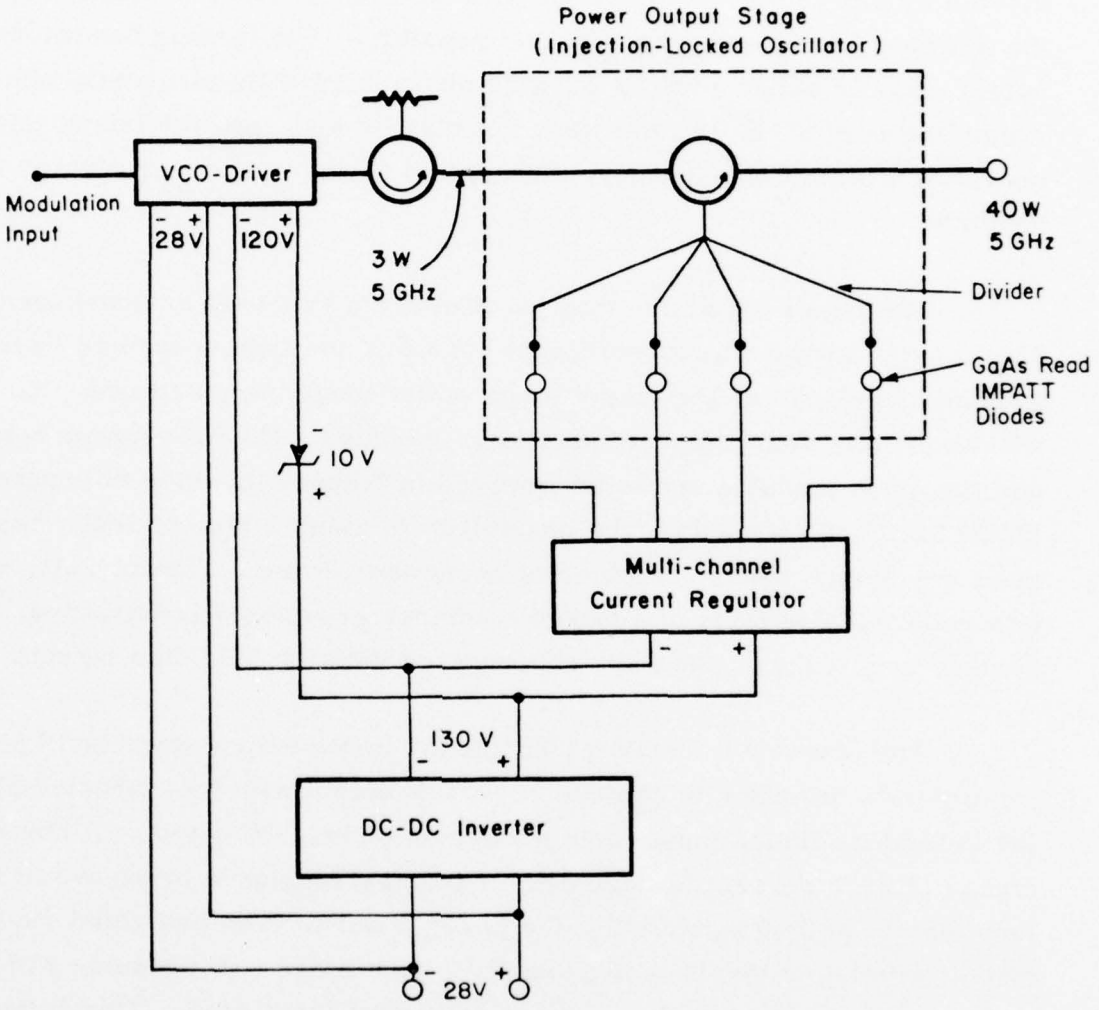

Figure 2-1 Functional Block Diagram of Transmitter as Presently Planned.

diodes operating as an injection-locked oscillator in a parallel-type power-combiner circuit. A five-diode stage had originally been planned. However, it was found that diodes with more than 15-W CW output each could be fabricated by increasing the diode junction area from that previously used, so the simpler four-diode stage became possible. The locking bandwidth of the output stage is expected to be greater than the 10-MHz electronic tuning range required of the transmitter, but may be less than the full 60-MHz operating band. Consequently, mechanical tuning of the output stage may be required.

The power combiner may be of either a resonant or nonresonant type. At present, a nonresonant multiport hybrid of the type described by Gysel[5] is being developed as the output stage power-combining network. To this will be coupled four separate oscillator modules. Both the power combiner and the diode modules are to be realized in trapped inverted microstrip (TIM) line.[6] As a backup, the possibility of using a dielectrically loaded resonant-cavity power combiner is being considered. This circuit, which is a reduced-size form of a power combiner previously constructed,[3] will be used only if difficulties are encountered with the TIM-line circuit.

The projected combining efficiency in the output stage is 70 percent (minimum). In order to achieve 40-W CW output with this circuit efficiency, the individual diodes must each be capable of 14.7-W output. A diode efficiency of 26.5 percent is assumed. Diode performance in excess of this level has been demonstrated in the present work. The projected diode and circuit efficiency levels imply that the output stage will consume 215 W at the nominal 105-to-110-V operating voltage of the diodes. This is less than the 232 W originally budgeted, and partially offsets the overrun in power consumption in the VCO-driver subassembly.

A circulator, not originally included, is shown between the VCO-driver and the output stage. This may be required to prevent undesired interaction between the driver and the output stage, particularly in the case where the transmitter operates into a mismatched load.

Including the circulator, which provides an additional 20 dB (nominal) isolation, should insure that the last stage in the driver always locks to the Gunn VCO frequency as desired, rather than to the free-running frequency of the output stage, even with output load VSWR's as great as 2:1.

The multichannel current regulator provides four individually adjustable current-regulated bias outputs to operate the diodes in the power output stage. This regulator is an extension of the single-channel regulator developed during the previous program.[2] While the regulator consumes essentially no current, there is a voltage drop of 15 to 20 V across the circuit during operation. Overall system efficiency can be improved if this voltage drop can be reduced. The change from a five-diode to a four-diode output stage has simplified the design of the current regulator significantly.

The DC-to-DC inverter produces 130-V DC nominal output from the 28-V DC primary power for operation of the IMPATT diodes in the VCO-driver subassembly and in the output stage. (The Gunn oscillator in the VCO-driver is operated directly from the 28-V primary power source through a voltage regulator.) The inverter output voltage was raised from the 120 V originally planned to accommodate the higher operating voltage of the recently fabricated high-power GaAs Read IMPATT diodes. To achieve lower overall cost and to avoid spending a large part of the program effort in power supply development, a standard, commercially available inverter is to be used. The unit selected offers a conversion efficiency of up to 80 percent, but exceeds the size and weight goals for the entire transmitter package. Possibilities for reducing the size and weight of the inverter and for obtaining still higher efficiency are being pursued with the manufacturer. Using the present inverter, the total load current imposed on the 28-V primary power source by the complete transmitter package will be ~15 A.

3.0 DEVELOPMENT OF TRANSMITTER COMPONENTS

3.1 VCO-Driver Subassembly

The VCO-driver subassembly is essentially a 3-W CW FM transmitter which operates at 5 GHz. Power consumption of this subassembly is relatively small compared with that of the complete 40-W transmitter. Consequently, little improvement in overall transmitter efficiency can be obtained by refining the VCO-driver subassembly.

The performance required from the VCO-driver is similar to that of sources and amplifiers produced routinely by the Raytheon Special Microwave Devices Operation (SMDO) using established IMPATT and Gunn diode technology. For this reason, and because little was to be gained in transmitter efficiency by exploiting new technology in this subassembly, the unit was ordered from SMDO. The VCO-driver subassembly was received in final form from SMDO in September 1976.

The specifications established for the VCO-driver subassembly were derived from the performance objectives of the present transmitter and from experience gained during the previous program[2]. The unit was to operate at 5 GHz with a ±30 MHz available frequency adjustment. Power output variations in the driver have little effect on the output of the transmitter since the subsequent 40-W output stage operates as a high-gain injection-locked oscillator. However, it was considered desirable to maintain the driver power output within 1 dB of the nominal output across the operating band. The driver was to have the same FM capability required in the transmitter as a whole: a 10-MHz peak-to-peak deviation capability with power not less than 1 dB below the maximum at any point, and 10-MHz modulation frequency capability with modulation sensitivity not less than 1 dB below the mid-band level.

Power output for the driver was specified at 3 W. In previous work[2], 330 mW of drive had provided 6 MHz of locking bandwidth with a 60-W high-Q multiple-diode output stage. Since locking bandwidth varies as $(1/Q_e)\sqrt{P_\ell/P_o}$, 3 W should provide more than 20 MHz of locking range, even if the new output

stage operates at the same external Q. The nonresonant power combiner presently planned should be lower in Q and should permit still greater locking bandwidth. Thus, 3-W output from the driver should provide positive injection locking over the 10-MHz band required in the complete transmitter. It may not, however, provide 60 MHz of locking, which would permit the entire operating band of the transmitter to be covered without mechanical retuning of the output stage.

The VCO-driver subassembly was to operate from power available in the transmitter package: 28 VDC primary power and 120 VDC from the DC-to-DC inverter for the IMPATT diodes. Total power consumption was budgeted at 33 W. Analysis of the reliability of the components included was to insure that the 5000-hour operating life and 7-year shelf-life requirements for the entire transmitter would not be adversely affected by the driver. Original plans called for the subassembly to fit within a 3.5" x 4" x 1" volume and weigh less than 1 lb.

Since the subsequent output stage operates as an injection-locked oscillator, the overall FM noise of the transmitter is largely determined by that of the VCO-driver. By requiring that the total noise from the driver in a 1-kHz bandwidth 100 MHz from the carrier be at least 40 dB below the carrier, we can insure that the -30 dBC transmitter noise specification is met with a considerable margin.

Figure 3-1 shows a functional block diagram and a schematic mechanical layout of the VCO-driver subassembly as it was finally received. It consists of a Gunn diode VCO followed by two IMPATT diode amplifier stages, which operate in the injection-locked oscillator mode. Interstage and output circulators are used to prevent undesired interactions between stages or with the subsequent transmitter output stage. The Gunn diode is operated from the 28-V primary power supply through a voltage regulator. The current regulator for the IMPATT diodes accepts 120-V input, which is derived from the DC-to-DC inverter.

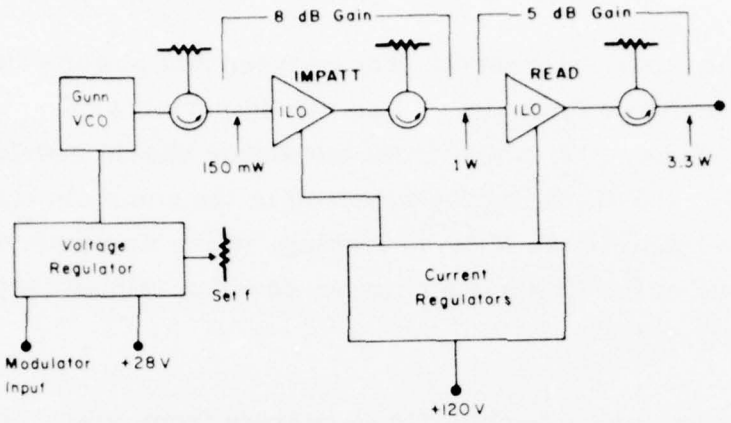

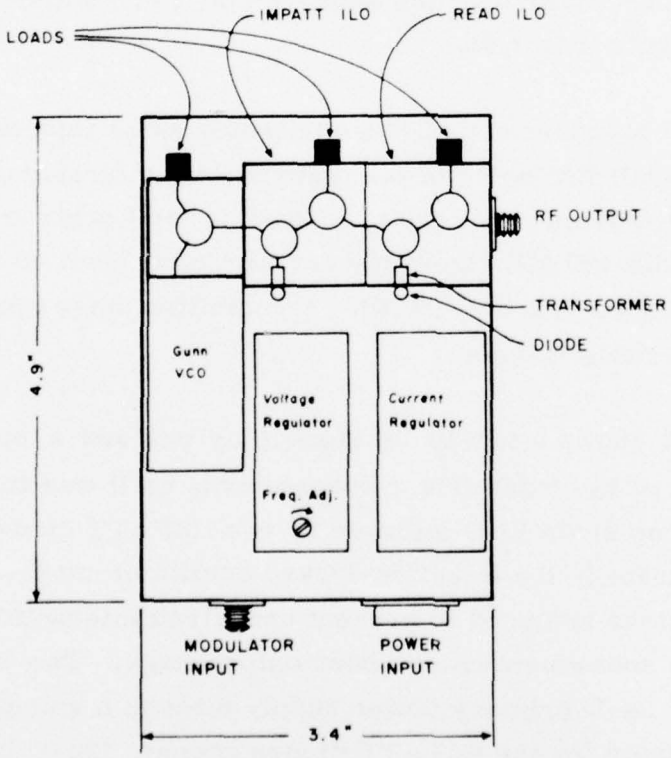

Figure 3-1 Functional Block Diagram and Schematic Mechanical Layout of the VCO-Driver Subassembly.

The Gunn oscillator stage produces 150-mW output at 5 GHz. Tuning over the 4.97-to-5.03-GHz range is accomplished by variation of the operating bias voltage. Frequency modulation is also accomplished by an independent variation of bias voltage. The modulation is AC-coupled to the bias voltage regulator, so there is a low-frequency cutoff of the modulation sensitivity. This has been set to ~70 kHz, which is acceptable in many FDM-FM systems. The use of bias tuning and bias modulation results in some variation in the output amplitude of the oscillator across the operating band. This variation is less than 1 dB and is relatively unimportant because succeeding stages operate as high-gain injection-locked oscillators with saturated power output. Bias tuning was chosen because it provides a simpler RF circuit than could be realized with varactor tuning.

The first IMPATT stage uses a flat-profile GaAs diode operating as an injection-locked oscillator. Locking is maintained across the full 4.97-to-5.03-GHz operating band without mechanical retuning. The stage produes 1-W output with 100-mW input at 5 GHz.

The second IMPATT stage uses a GaAs Read diode operating as an injection-locked oscillator. Locking is maintained across the full 4.97-to-5.03-GHz operating band without mechanical retuning. The stage produces 3-W (nominal) output with 1-W input at 5 GHz.

Performance of the complete VCO-driver subassembly is summarized in Table 3-1. While the gain distribution and power levels of the stages differ somewhat from those originally proposed, the RF performance is satisfactory. Power output exceeds 3 W across the 4.97-to-5.03-GHz operating band. Total power consumption is ~61 W, substantially larger than the 33 W originally budgeted. The size and weight of the package are also larger than originally planned, although if the base plate is considered as part of the main heat sink for the transmitter, the size and weight overruns are small. Planned and actual performance characteristics are compared in Table 3-2.

TABLE 3-1

VCO-DRIVER PERFORMANCE

Nominal Operating Conditions:

IMPATT diodes	-	120 VDC
		350 mA
Gunn diode	-	28 VDC
		670 mA

Power Output:

f(GHz)	P_o(W)
4.97	3.16
4.98	3.31
4.99	3.46
5.00	3.54
5.01	3.54
5.02	3.54
5.03	3.54

TABLE 3-2

COMPARISON OF PROPOSED AND ACTUAL
VCO-DRIVER SUBASSEMBLY CHARACTERISTICS

PROPOSED	ACTUAL
Power Output 3 W, 4.97-5.03 GHz	Power Output 3.3 W (Typical), 4.97-5.03 GHz
Size 3.5 x 4 x 1 $in.^3$	Size 3.75 x 4.88 x 1.25 $in.^3$ (Top compartment only) 4 x 5.75 x 1.45 $in.^3$ (Overall, including base plate)
Weight ~1 lb	Weight 1.11 lb (Top compartment) 1.67 lb (Total, including base plate)
Power Consumption 120 V, 200 mA 28 V, 300-350 mA ~33 W Total	Power Consumption 120 V, 350 mA 28 V, 670 mA ~61 W Total

The VCO-driver subassembly was ready for integration with the remaining transmitter components at the end of the period covered by this report. A photograph of the completed subassembly is shown in Fig. 3-2.

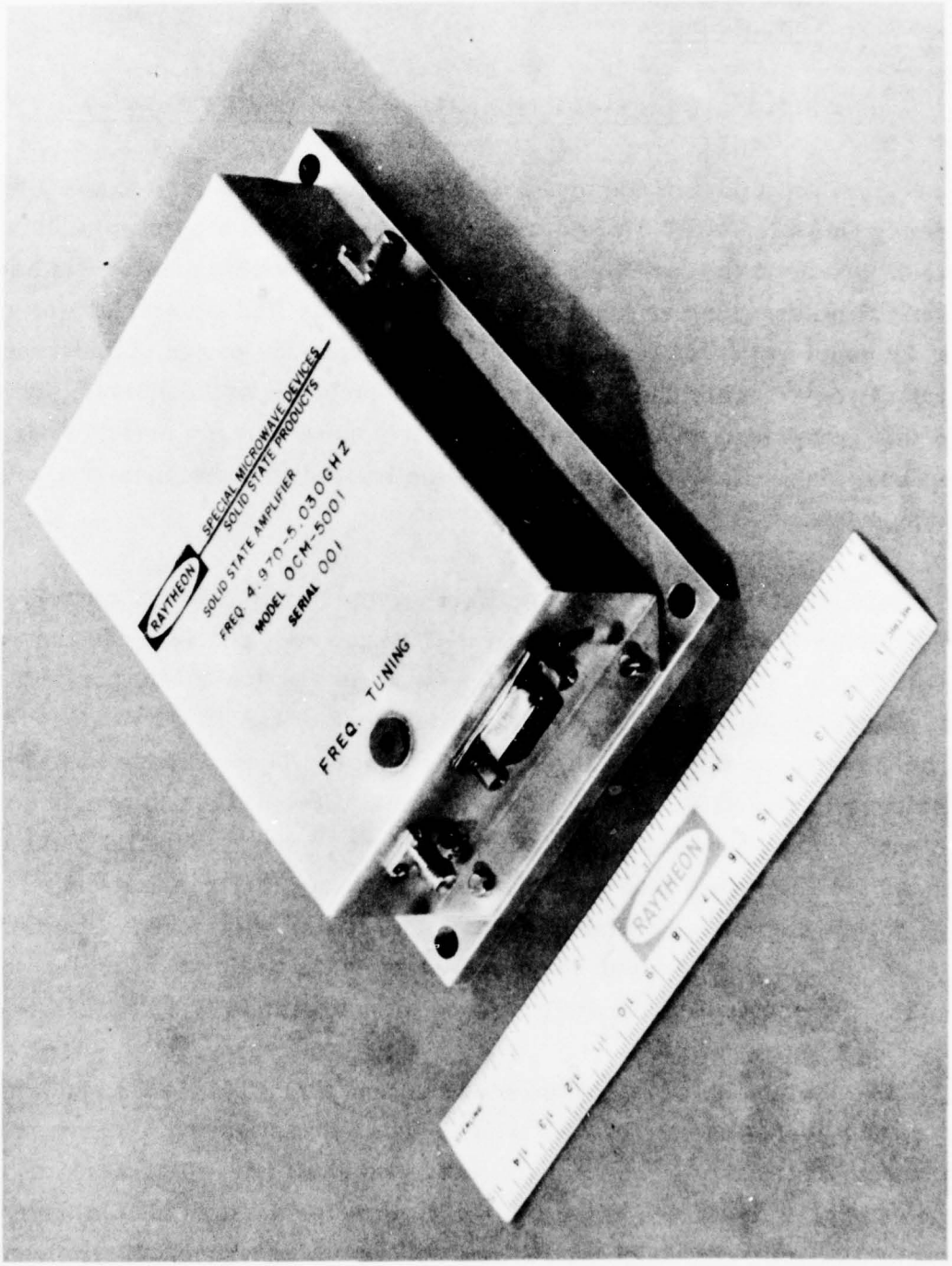

Figure 3-2 Photograph of the Completed VCO-Driver Subassembly

3.2 Output Stage

3.2.1 High-efficiency GaAs Read IMPATT diodes

As a part of the previous RADC program,[2] high-power, high-efficiency GaAs IMPATT diodes capable of operation at 5 GHz were developed. These diodes used the low-high-low modified Read doping profile and had platinum Schottky-barrier junctions. The required GaAs material was produced by vapor phase epitaxial growth. For improved power output, reduced electrical series resistance, and reduced thermal impedance, each high-power diode was comprised of four mesas in a 2×2 square array on an integral gold plated heat sink. Each four-mesa chip was bonded into a standard microwave diode package.

With diodes operating as oscillators, the best performance achieved in the previous work was 13.3-W CW output with 24 percent efficiency in the 4.8-4.9 GHz range. Diodes from two different wafers reached this performance level. More typical of the better diodes fabricated was 10-11 W CW output with 22-23 percent efficiency in the 5-GHz range. These diodes had thermal resistances in the range 4.5-5.0^{o}C/W, which allowed them to produce their rated power output with junction temperatures of ~200^{o}C. Initial plans called for the use of five such diodes in the output stage of the transmitter. The design for these diodes is well in hand. This is demonstrated by the fact that eleven of thirteen epitaxial wafers selected for device processing toward the end of the previous program produced diodes with 10 W or more CW output.[3]

The reliability of high-power GaAs Read IMPATT diodes, both under storage and operating conditions, is still under investigation. There is no apparent fundamental or inherent limitation on shelf life. The work of Coleman et al.[7] indicates that Pt Schottky-barrier devices should have operating lifetimes approaching 10^5 and 10^4 hours with junction temperatures of 180^{o}C and 230^{o}C, respectively. Our own work on multilayer (Pt-Ti-Au) Schottky-barrier metallization for low-high-low Read diodes indicates that lifetimes

in excess of 10^5 hours should be possible at junction temperatures of 200°C. In all cases, the limitation on lifetime occurs because of the ongoing chemical reaction between the GaAs material and the Schottky-barrier metallization. The presently achievable reliability should meet the requirements of the transmitter. While no detailed reliability study was planned as part of the present program, such additional reliability data as becomes available will be used in projecting the lifetime of the final transmitter design.

The present program includes no diode development effort. The high-power GaAs Read diodes required both for the transmitter and for the incidental monthly diode deliveries were to be produced using existing technology, namely, that technology used during the previous program. This technology, including material growth, diode fabrication, and diode evaluation, was described in the final report of the previous program.[3]

Material growth and diode fabrication procedures are continually being refined in our laboratory as the result of a number of ongoing IMPATT diode programs. For this reason, there are several differences between the diodes produced for this program and those developed for the previous program. First, silicon (as SiH_4) rather than sulfur (as H_2S) is used as the n-type dopant during vapor phase growth of the GaAs epitaxial material. Silicon does not diffuse as rapidly as sulfur in GaAs, and silicon doping allows more precise control of the doping profile. Also, silicon-doped buffer layers of lower resistivity than those produced with sulfur doping can be obtained. This reduces the series resistance of any IMPATT diode and increases efficiency. Second, the doping profile specifications for the new diodes were refined based on experimental results obtained toward the end of the previous program. The changes involved an increase in electric field step and a decrease in drift region doping to raise the diode efficiency. Clearly, diode efficiencies of 25 to 30 percent, instead of 20 to 25 percent as typically obtained in previous work, would improve the overall transmitter efficiency. Third, a gold-germanium ohmic back contact has now been adopted as standard for all of our IMPATT diodes. This results in somewhat lower series resistance for higher efficiency, and somewhat more repeatable

diode characteristics than could be achieved with the previous chrome-gold back contact. Finally, by comparison of the older C-band diodes with X-band diodes produced for another program, it became evident that the junction areas of the early C-band diodes were quite small compared with the maximum which could be tolerated in typical circuits. Accordingly, the diameters of the mesas on the four-mesa chips were increased to 10 mils from the 7-8 mils used previously. This change permitted power outputs of 15 W (nominal) from each diode package. A four-diode output stage, having simpler bias and RF circuitry than would be used in the five-diode output stage originally proposed, then became possible.

The general form of the low-high-low doping profile used in the high-power diodes is shown in Fig. 3-3, along with the electric field profile present in the reverse-biased diode. Notation for Fig. 3-3 is explained in Table 3-3. The doping profile specification to which the material was grown is shown in Table 3-4. The initial specifications were refined during the course of the work, as will be described.

An epitaxial reactor was calibrated for the growth of C-band wafers, and the first wafer was delivered to the specifications of Table 3-4. during April 1976. A total of six wafers was delivered during the April-through-June time period. Diode processing was started on these wafers as they were received. Toward the latter portion of the growth series, recurring problems with poor wafer surfaces were encountered. These were eventually traced to a small leak in the reactor tube, which was repaired. This first reactor was then dedicated to other programs. A second epitaxial reactor was calibrated for C-band growth during September 1976. This reactor, working to the modified specifications shown in Table 3-4. was to be used to grow the remaining wafers required for the program.

By the end of September 1976, diode fabrication and RF testing of sample units from the first six wafers had been completed. A four-mesa plated-heat-sink chip typical of those used in the diodes is shown in Fig. 3-4. Ten-mil-diameter mesas are mounted on 20-mil centers.

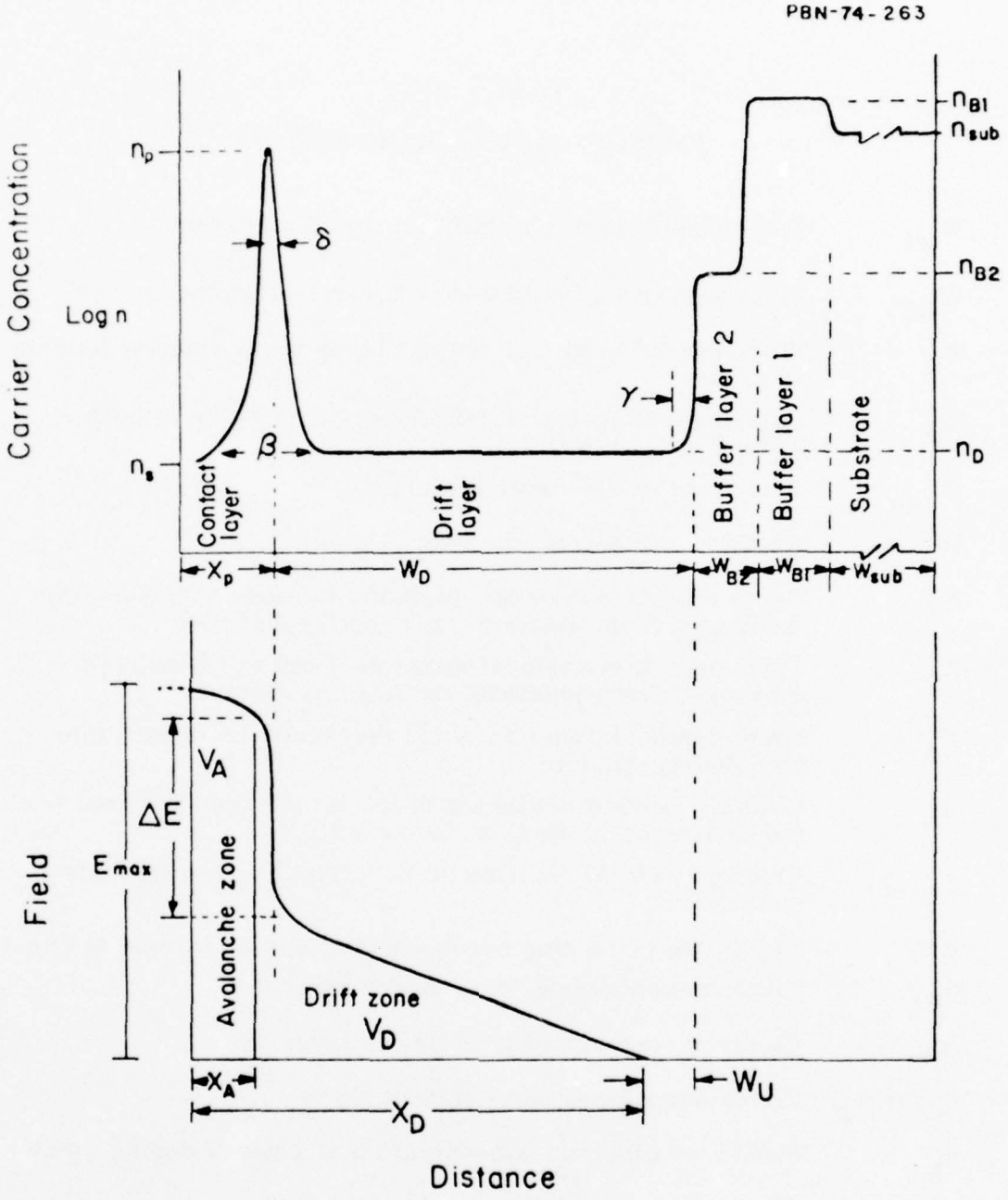

Figure 3-3 Schematic Representation of the Donor-Density Profile and the Electric-Field Profile of a Stepped-Field (LHL) Read Diode. The notation used in this figure is identified in Table 3-3.

TABLE 3-3

IDENTIFICATION OF NOTATION

W_{B1}	Thickness of epitaxial buffer layer 1 as grown
W_{B2}	Thickness of epitaxial buffer layer 2 as grown
W_C	Thickness of epitaxial contact layer from spike to surface as grown
W_D	Thickness of epitaxial drift layer from spike to buffer layer 2 as grown
W_{sub}	Thickness of substrate material
W_u	Width of undepleted epi zone in diode
X_A	Depth of avalanche zone-distance in diode at breakdown measured from junction, or Schottky barrier
X_D	Total depletion depth-distance in diode at breakdown measured from junction, or Schottky barrier
X_p	Spike depth-distance in diode measured from junction, or Schottky barrier
E_D	Electric field at beginning of the linear field portion of the drift zone in diode at breakdown
E_{max}	Electric field at junction or Schottky barrier in diode at breakdown
ΔE	Field step occurring across doping spike in diode at breakdown
n_{B1}	Electron concentration of buffer layer 1
n_{B2}	Electron concentration of buffer layer 2
n_D or n_2	Electron concentration of drift layer
n_p	Measured electron concentration at peak of doping spike
n_{sub}	Electron concentration of substrate
n_S or n_1	Electron concentration measured with zero bias applied to junction or Schottky barrier
β	Base width of doping spike measured at 1.5 n_D
δ	Full width of doping spike measured at half height (0.5 n_p)
γ	Width of doping transition from drift layer to buffer layer 2

TABLE 3-4

SPECIFICATIONS FOR 5 GHz READ WAFERS

W_{sub}	~400 micrometers (*thinned in processing*)	$n_{sub} > 1 \times 10^{18}$ cm^{-3}
W_{B1}	5-10 micrometers	$n_{B1} \sim 2 \times 10^{18}$ cm^{-3}
W_{B2}	~1.5 micrometers	$n_{B2} \sim 2 \times 10^{16}$ cm^{-3}
W_D	8-10 micrometers (preferably ~9)	$n_D \sim 2.5 \times 10^{15}$ cm^{-3}
X_p	~0.25 micrometers	$n_s < 2 \times 10^{16}$ cm^{-3}
δ	~0.04 micrometers	$n_p \sim 4.8 \times 10^{17}$ cm^{-3}
ΔE	~3.3×10^5 V/cm	

CHANGES TO BE IMPLEMENTED IN FUTURE GROWTH RUNS

W_D = 9-11 micrometers (preferably ~10)

X_p = 0.26 micrometers

ΔE = $3.0\text{-}3.3 \times 10^5$ V/cm

n_D = $2.0\text{-}2.4 \times 10^{15}$ cm^{-3}

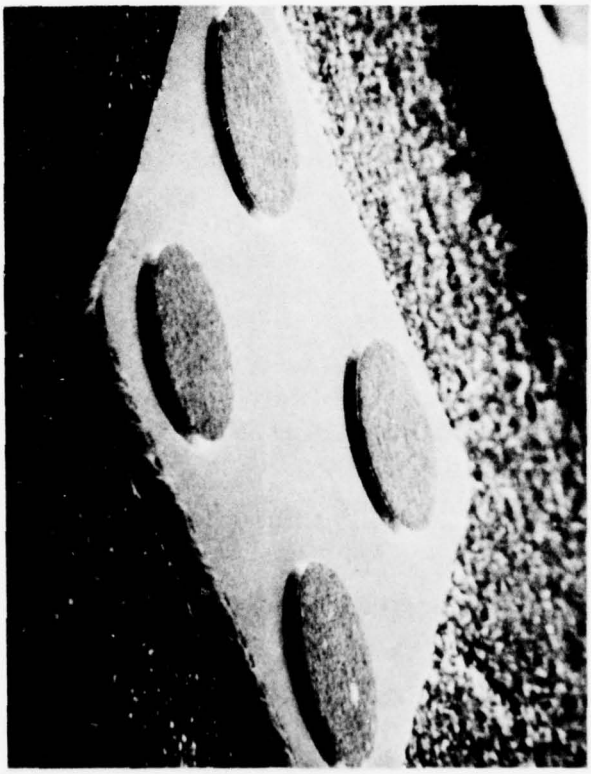

Figure 3-4 Scanning Electron Micrograph of a Four-Mesa PHS Diode Chip.

The completed chip is approximately 40 mils square. The chips were soldered into microwave packages, and gold mesh was used to contact the mesa tops as is shown in the cut-away view of Fig. 3-5. Lids were welded on the packages to complete a hermetic seal of each diode.

Table 3-5 shows the best results obtained through the end of September in CW oscillator tests of all six diode lots. In all cases, the diodes used four-mesa PHS chips with 10-mil-diameter mesas. Thermal resistances were typically $4^{o}C/W$, and maximum powers were achieved with junction temperatures in the 200 to $220^{o}C$ range. Where "best power" and "best efficiency" occurred under substantially different conditions, both results are listed. A "top-hat" oscillator circuit of the type shown in Fig. 3-6 was used for these tests.

TABLE 3-5

BEST RESULTS IN CW OSCILLATOR TESTS

Diode Lot	Wafer	P_o(W)	f(GHz)	η(%)
904	81905	12.83	6.510	23.3
905	81907	14.88	5.835	26.2
906	81908	15.38	5.735	26.9
907	81910	18.21	5.247	25.7
		15.89	5.696	26.7
909	81915	21.01	4.861	29.5
910	81934	17.55	4.874	28.4

The results obtained indicate that the wafer selection criteria used were adequate for producing diodes with the power and efficiency levels required in the transmitter output stage. Five of the six diode lots contained units which reached or exceeded the 15-W (nominal) power output level.

Figure 3-5 Four-Mesa Diode Packaged with Crossed-Mesh Connections.

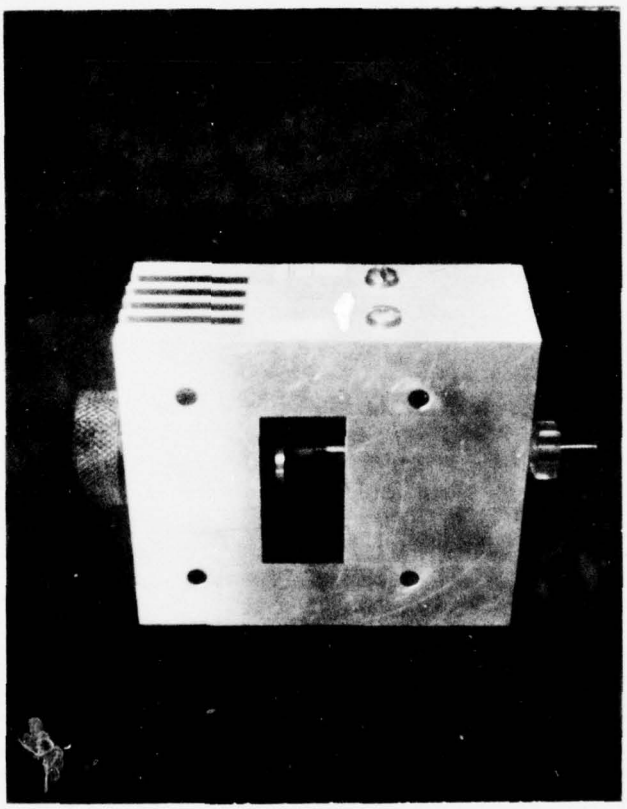

Figure 3-6 C-Band Top-Hat Oscillator

The efficiencies of these diodes also exceeded 22-23 percent, which had been typical during the previous program.[2] The spread of preferred operating frequencies was greater than desired, however, and operating frequencies tended to be greater than 5 GHz. The doping profile changes indicated in Table 3-4 were implemented to correct this situation in the remaining wafer growth runs to be made during the program.

The results from lot 909 are particularly interesting. Through the end of September, 46 diodes had been made from the wafer. Of these, sixteen survived CW oscillator tests. All of the survivors produced more than 18-W CW output. Also, eight diodes of the sixteen produced more than 20-W CW output. Thus, while the 20-W diode must still be regarded as an experimental device, it is more than a one-of-a-kind accident. Further, diodes producing 15 W with about 25 percent efficiency can be fabricated in sufficient quantities to complete the transmitter output stage in the four-diode configuration planned.

3.2.2 The power-combining circuit

3.2.2.1 General circuit types and operating modes

While circuits for combining the power outputs of microwave diodes may take a number of different forms, they usually belong to one of two general classes, the tandem and parallel power combiners. These two types are illustrated in Fig. 3-7. The tandem power-combining circuit is a succession of low-gain amplifier or injection-locked oscillator stages containing equivalent IMPATT diodes. The earlier stages in the chain are adjusted for higher gain and the later stages for lower gain so that each stage contributes to the ongoing signal the maximum power which its diode can produce. This type of combiner tends to be severely limited by circuit losses, particularly in the later stages, where the power consumed by a fraction of a decibel of loss can approach the power contribution of the diode. Because of this loss limitation, the tandem power combiner was not selected for use in the deliverable transmitter. The parallel power combiner is a single reflection amplifier or injection-locked oscillator stage with multiple active elements. Circuit losses tend to accumulate less rapidly in this type of circuit than they do in the tandem power combiner. The power-combining circuits considered for use in the deliverable transmitter are all of the parallel type.

There are two general types among the parallel power combiners. In the resonant power combiner, there is a single resonator to which an ensemble of diodes is coupled and from which the output power is extracted. In the nonresonant power combiner, an ensemble of oscillators, each with its own resonator, is locked to a common reference signal and coupled to a single output port through a broad-bandwidth multiport hybrid circuit. Both resonant and nonresonant power combiners were considered for use in the deliverable transmitter.

PBN-74-233

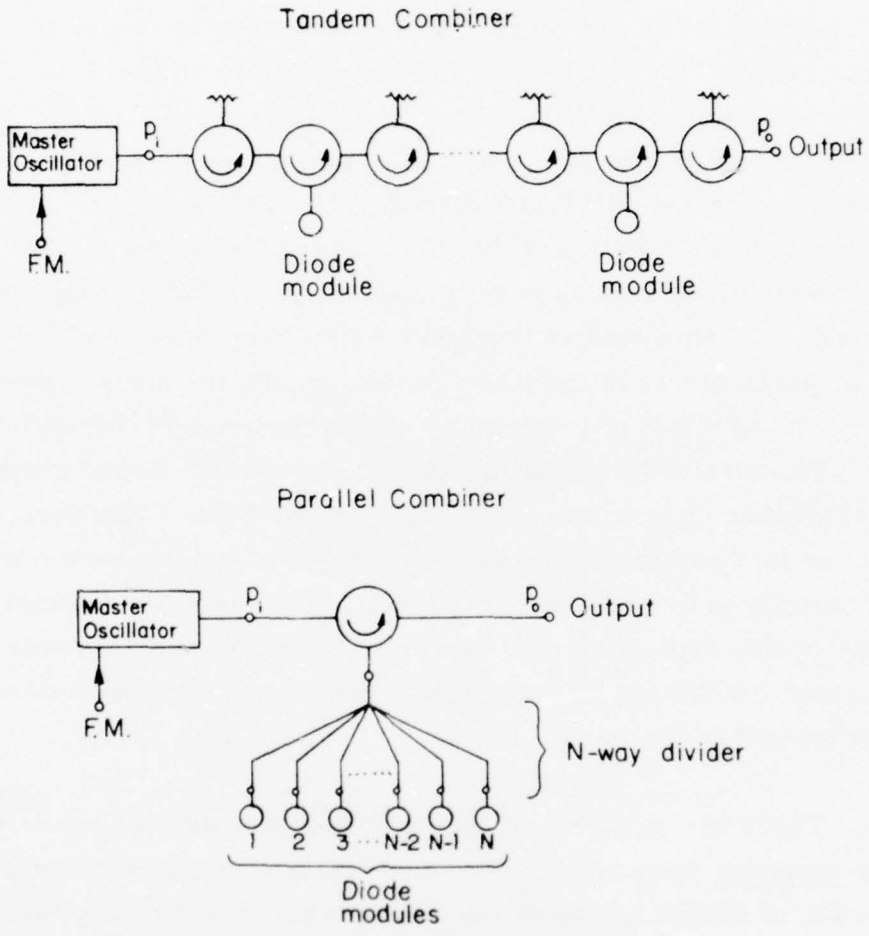

Figure 3-7 Two Basic Types of Power Combiner. Each is shown combined with a low-power master oscillator having FM capability to produce a complete transmitter.

3.2.2.2 Circuit requirements and performance limitations

There are two principal factors which limit the performance of a power-combining circuit. The first is circuit loss which tends to reduce overall efficiency. The second is the presence of undesired modes of oscillation in the circuit which may be caused by insufficient diode-to-diode isolation in a nonresonant power combiner or by the presence of multiple resonances in a resonant power combiner. These limiting factors can be described in terms of the model shown in Fig. 3-8.

The circuit efficiency is a useful quantity for comparing the relative performance of different power combiners. This is defined as the net power contributed by the power combiner divided by the total power available from the diodes. With reference to Fig. 3-8, one can write $\eta = (P_o - P_i)/(NP_D)$. The circuit efficiency depends on the circuit loss and on the gain at which the power-combined stage operates. The special case of a power-combined, free-running oscillator is treated by allowing the stage gain to become arbitrarily large. Circuit efficiency as a function of loss with diode gain as a parameter is shown in Fig. 3-9.

In the present transmitter design, the output stage operates with somewhat more than 10 dB gain. The goal for the circuit efficiency in this stage is 70 percent. A conservative estimate of the maximum permissible circuit loss for which 70 percent circuit efficiency can be achieved can be found by using the G = 10 curve in Fig. 3-9. This shows that a total circuit loss of 1.2 dB can be tolerated. Since the loss of the circulator is likely to be ~ 0.4 dB per pass, a loss of 0.8 dB can be tolerated in the power combiner itself. Smaller losses will result in circuit efficiencies greater than 70 percent.

Stability against undesired modes of oscillation can be assured in the case of a resonant power combiner by using a cavity resonator which has only a single resonance in the band of frequencies where the diodes have appreciable negative resistance. When a relatively small number of diodes

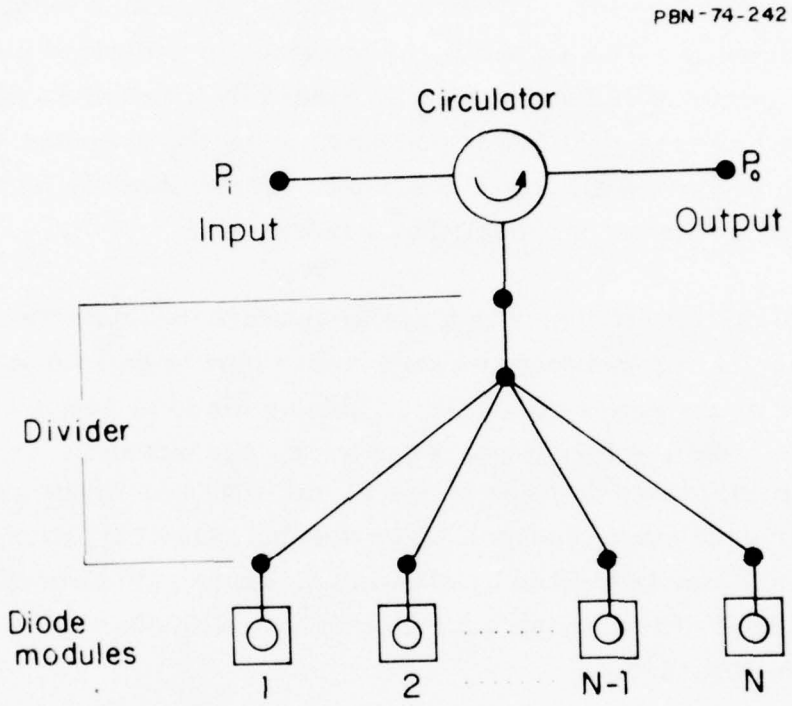

Figure 3-8 Model Used for Analyzing the Limitations of the Microwave Power Combiner. N identical diode modules, each capable of producing a power output P_D, are combined in a single stage.

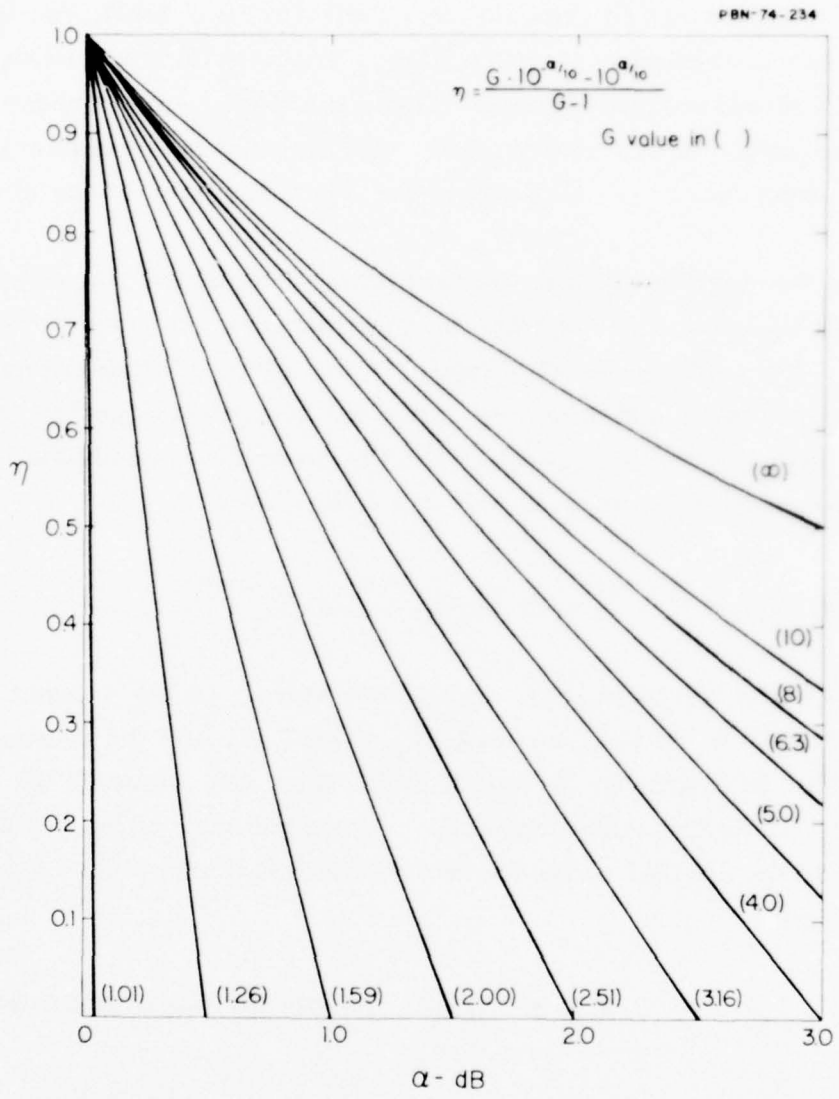

Figure 3-9 Circuit Efficiency as a Function of Circuit Loss with Diode Gain as a Parameter. α is the total power loss, expressed in dB, between the output port and the diode ports. The diode gain G is the square of the magnitude of the reflection coefficient at the diode ports.

is to be combined, as is the case here, the simplest technique for realizing single-mode operation is to use a TM_{010}-mode cylindrical cavity with a height of 0.3 wavelength or less. Then, the TM_{010}-mode resonance has the lowest frequency of any cavity mode, and the next mode is nearly 40 percent higher in frequency — well out of the operating band of the diodes.

In the case of the nonresonant power combiner, the stability requirement translates into a minimum permissible isolation between diode modules. Basically, at each diode port the desired locking signal, supplied by the VCO-driver subassembly, must be larger than the "interfering" signals, assumed uncorrelated, from the other diode modules. Defining α_i as the required isolation in dB, one finds that:

$$(P_i / N)\, 10^{-(\alpha / 10)} > (N-1)\, P_D \cdot 10^{-(\alpha_i / 10)}$$

is the condition for locking in the correct mode. In the present transmitter design, P_i = 3 W, N = 4, α = 1.2, P_D = 14.7 W, and the minimum isolation is 18.9 dB. In practice, an isolation substantially above 20 dB would be desirable. This isolation should be maintained over at least a 20 percent bandwidth, the normal range for which the diodes can produce substantial power output.

3.2.2.3 Circuit designs for the transmitter output stage

3.2.2.3.1 Dielectrically loaded cavity

During the previous program, six high-power GaAs IMPATT diodes were successfully combined in a resonant cavity circuit. When operated as a free-running oscillator, the circuit produced 62-W CW output at 5.120 GHz with 20.9 percent DC-to-RF conversion efficiency. It was successfully operated as an injection-locked oscillator with nearly 23 dB of locking gain.[3]

During the time period covered by this report, diodes from lots 907, 909, and 910 were successfully operated as single-diode oscillators in the old cavity. Power outputs were typically within 0.5 dB of the powers measured in our standard "top-hat" test oscillator. This demonstrated that impedance conditions suitable for the new 4× 10-mil-diameter mesa diodes could be provided in the cavity circuit.

The previous cavity circuit was too large and heavy to use in the present transmitter. One way to reduce the size of the circuit while retaining its high efficiency and single-mode characteristics is to fill the cavity with dielectric material. When material of dielectric constant $K \sim 4$ is used, the complete cavity circuit can be reduced to a cylindrical volume 1.7 inches in diameter and 3 inches long. The dielectrically loaded cavity is thus one form in which the new transmitter output stage could be realized.

Figure 3-10 is a schematic representation of the transmitter output stage using the loaded cavity. Four high-power GaAs Read IMPATT diodes are coupled to a common TM_{010}-mode cavity. Except for a small hole on axis and the cutouts required to pass the coaxial lines, the cavity is filled with dielectric. STYCAST 36 DA, manufactured by Emerson and Cuming, Inc., appears to be a suitable dielectric. This material has a dielectric constant of 3.7 and a loss tangent of 0.0007. The cavity frequency is controlled by the dielectric rod tuner, and output coupling is adjusted by moving the coaxial probe axially. Coupling of the diodes to the cavity is adjusted by changing the slug transformers and by moving the diodes axially. The required DC bias is supplied to the individual diodes along the coaxial center conductors which pass through lossy terminations in the top of the cavity structure. Cooling of the cavity can be provided, either by including an appropriate water jacket or by mounting the cavity against a cold plate.

The operating principles for the resonant cavity power combiner are now fairly well understood and have been described elsewhere.[3] The chief difference which will occur with the dielectric-filled cavity is a reduction in unloaded Q from ~5000 to ~1400 because of the losses in the

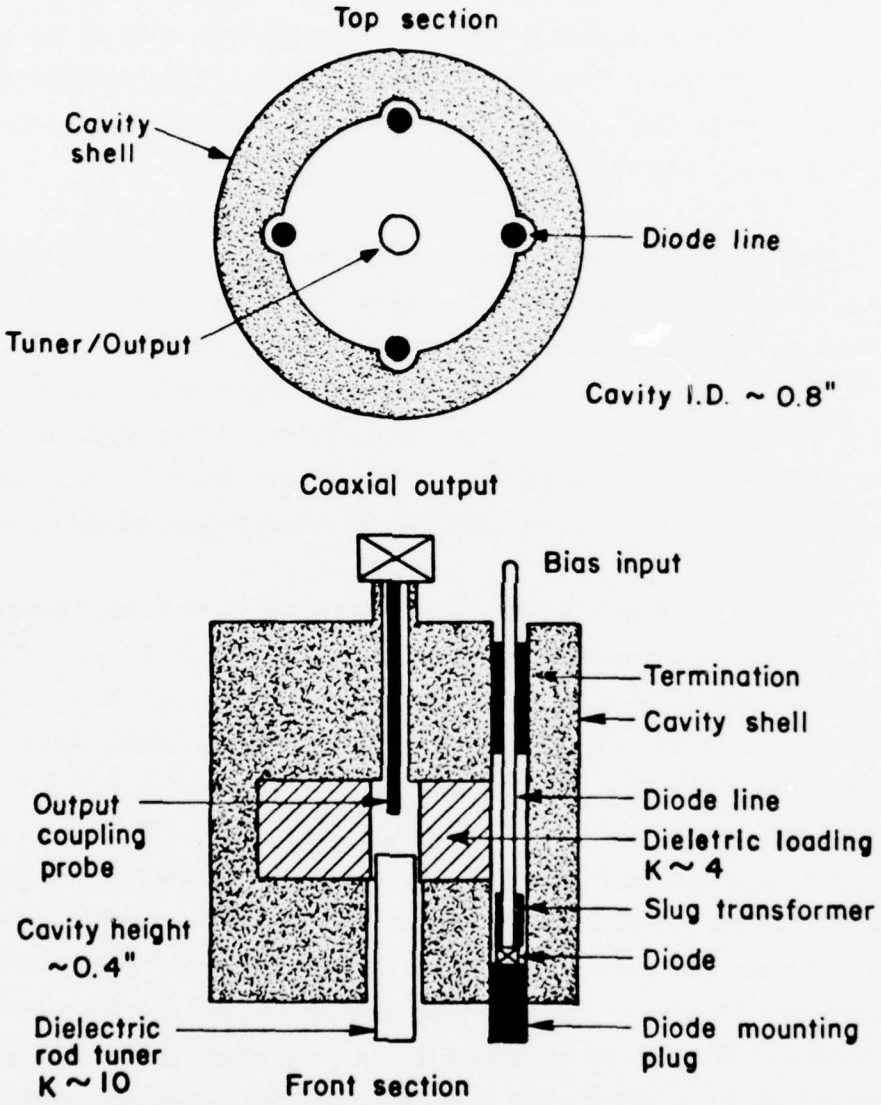

Figure 3-10 Schematic Representation of the Power Output Stage Using a Dielectrically-Loaded Cavity-Type Power Combiner.

STYCAST material. This will result in somewhat lower circuit efficiency and less freedom in the choice of cavity-coupling adjustments. However, the previous circuit operated with a loaded Q of ~100, less than 10 percent of the reduced unloaded Q, so less than 10 percent of the available power should be consumed in dielectric losses. This should still permit a circuit efficiency of at least 80 percent, since the full-size unfilled cavity had a circuit efficiency of ~90 percent.

The cavity circuit can meet the needs of this program and has a high probability of initial success based on our previous experience. However, it involves complicated machining and will probably be more expensive in production than the microstrip circuits to be described in the following section. For this reason, it is considered a back-up design to be pursued only if the microstrip circuit development encounters severe difficulties.

3.2.2.3.2 Nonresonant power combiners

3.2.2.3.2.1 Circuit types

Nonresonant power combiners can take one of several forms. These forms can usually be divided into two broad classes. In the first, the division of RF power from the output port back to the diode modules, is accomplished by cascading dividers, each of which has a relatively small number of ports. In the second class, the division is accomplished in a single multiport power divider/combiner. These classes are illustrated in Fig. 3-11.

The cascade of 3-dB hybrids allows the combination of 2^N diodes, where N is the number of levels in the cascade. Circuit losses tend to accumulate rapidly as the number of levels is increased. The practical limit for this type of circuit is reached when 8 or perhaps 16 diodes are combined. Initially, cascades of 3-dB hybrids were not considered for use in the transmitter output stage because a five-diode stage was planned. Since the present design includes a four-diode output stage, a two-level cascade of low-loss hybrids would be acceptable. It appears to be possible

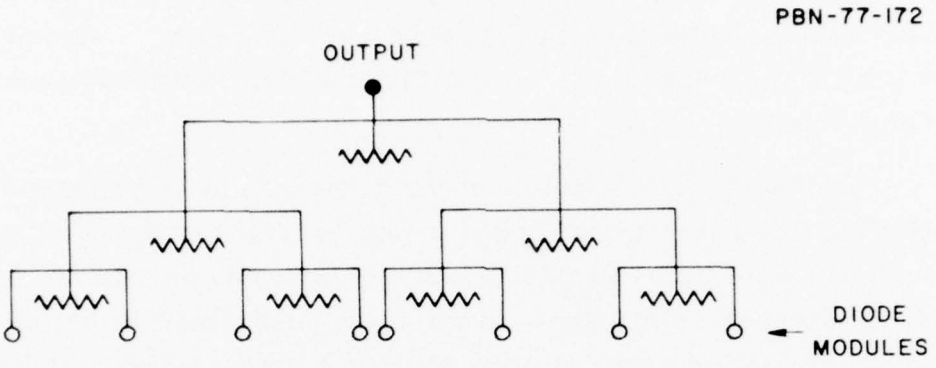

Figure 3-11 Nonresonant Power Combiner Types

to meet the 0.8-dB excess loss limit allowed for the power combiner when a circuit efficiency of 70 percent is required.

Several single-level nonresonant power-combining circuits have been considered for use in the transmitter output stage. These include the radial line, or "rising sun," combiner; the Wilkinson coupler,[4] and a modified Wilkinson coupler described by Gysel.[5] The radial-line circuit, shown in Fig. 3-12, was the output stage combiner originally proposed. It has the advantage of relatively simple fabrication with the number of diode ports not restricted to 2^N. However, there are a number of disadvantages of the circuit. It is difficult to achieve adequate isolation between the diode ports; the radius of the circuit is large ($\sim$ 6 wavelengths); the line segments become quite wide, leading to moding problems, when small numbers of diodes are combined; and the power-dissipating capability of the thin-film resistive material, which must absorb the power unbalance among diode modules, is limited.

The Wilkinson and Gysel circuits are potentially more compact than the radial-line circuit, since they are composed of quarter-wavelength line segments. The arrangement of each circuit for the case of two output ports is shown in Fig. 3-13. Both can give adequate performance in terms of loss and isolation. However, the Gysel circuit offers one particular advantage where high-power diodes are to be combined. The terminating resistors Z_T, which must dissipate any power unbalance between the diodes, are connected from line to ground. They can be high-power loads placed at the end of transmission line segments of characteristic impedance Z_T, thus removing them from the center of the circuit. Since power unbalances of several watts can occur in the event of a diode failure, high power loads are required in the present application. In the Wilkinson circuit, the termination is connected from line to line. Small chip resistors are commonly used for this purpose in microstrip circuits. These resistors have limited power-dissipating capability and would be unsuitable for the present application. Actual circuits of the Wilkinson and Gysel types are shown in Figs. 3-14 and 3-15 to demonstrate this difference in the terminations.

PBN-74-244

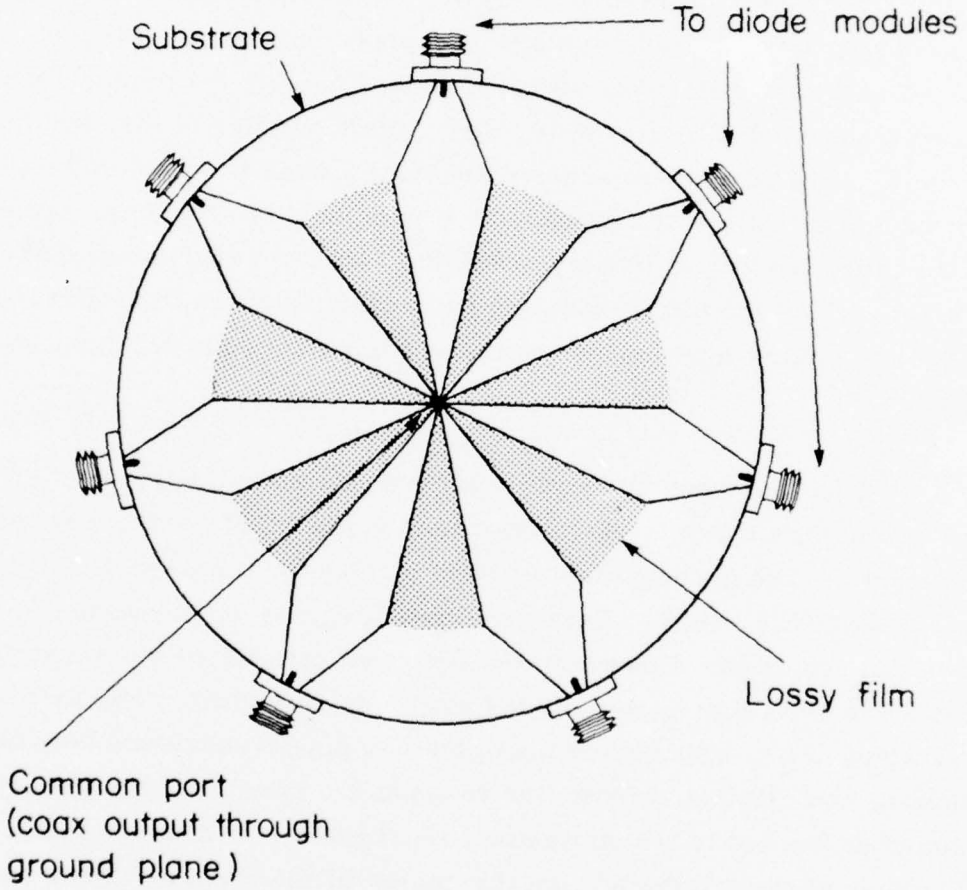

Figure 3-12 Microstrip N-Way Power Divider of the "Radial Line" Type.

PBN-77-171

WILKINSON-TYPE HYBRID

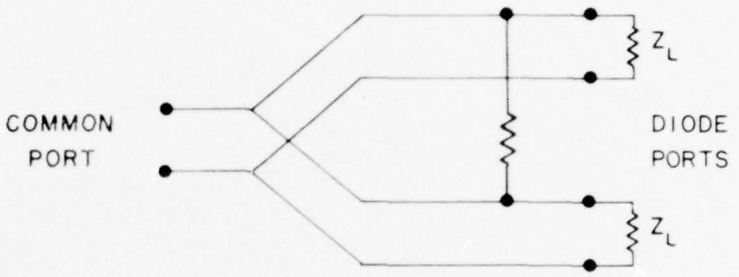

GYSEL-TYPE HYBRID

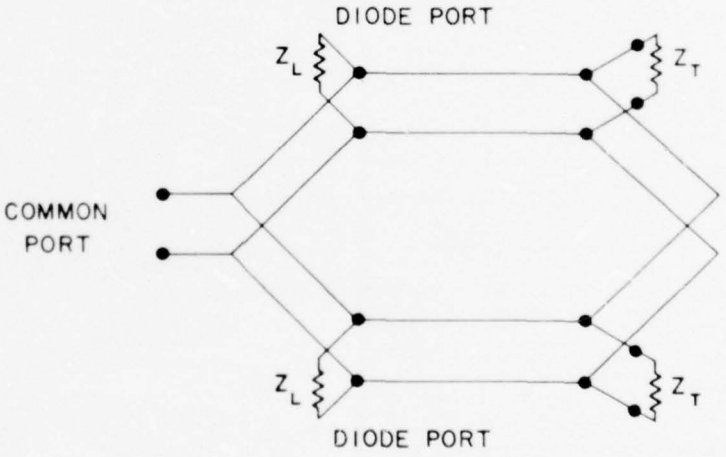

Figure 3-13 Transmission Line Configurations for Wilkinson and Gysel Hybrids with two Output Ports.

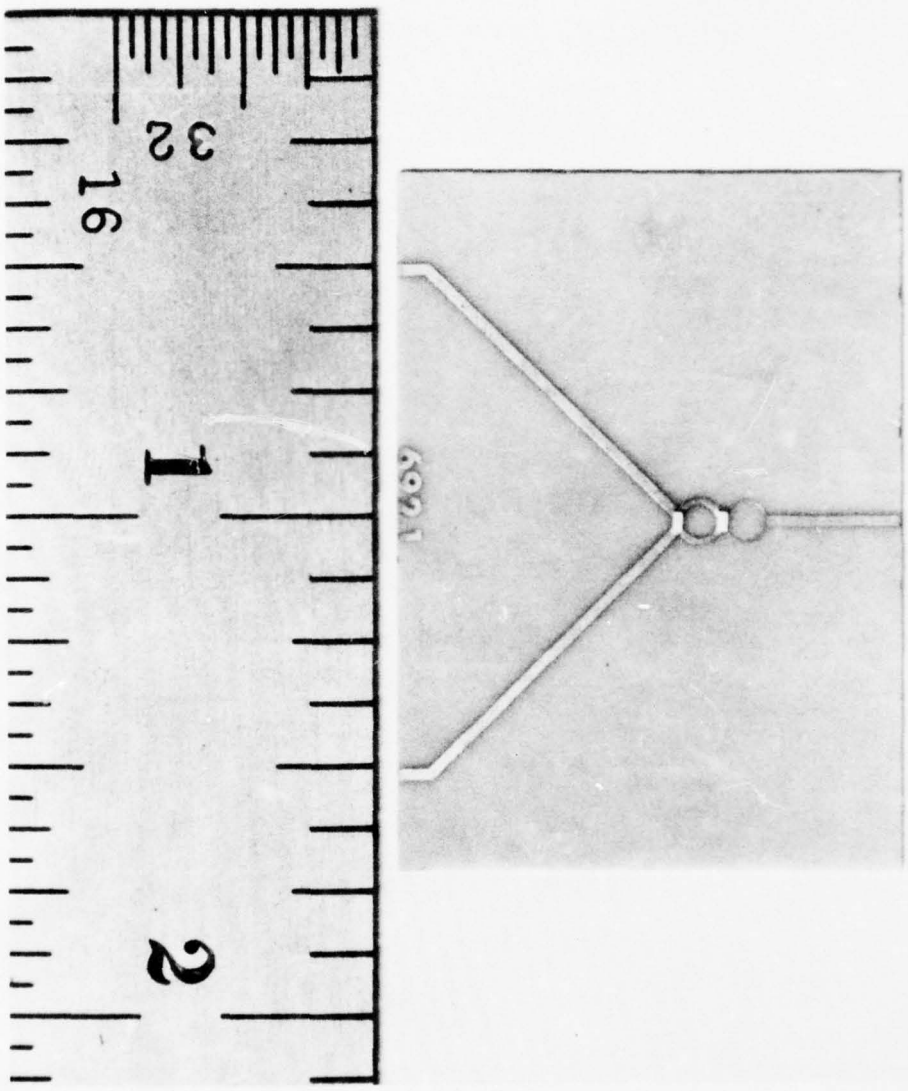

Figure 3-14 Wideband Two-Port Wilkinson Hybrid in Microstrip Configuration. In this double-section circuit, the terminations are small chip resistors connected from line to line.

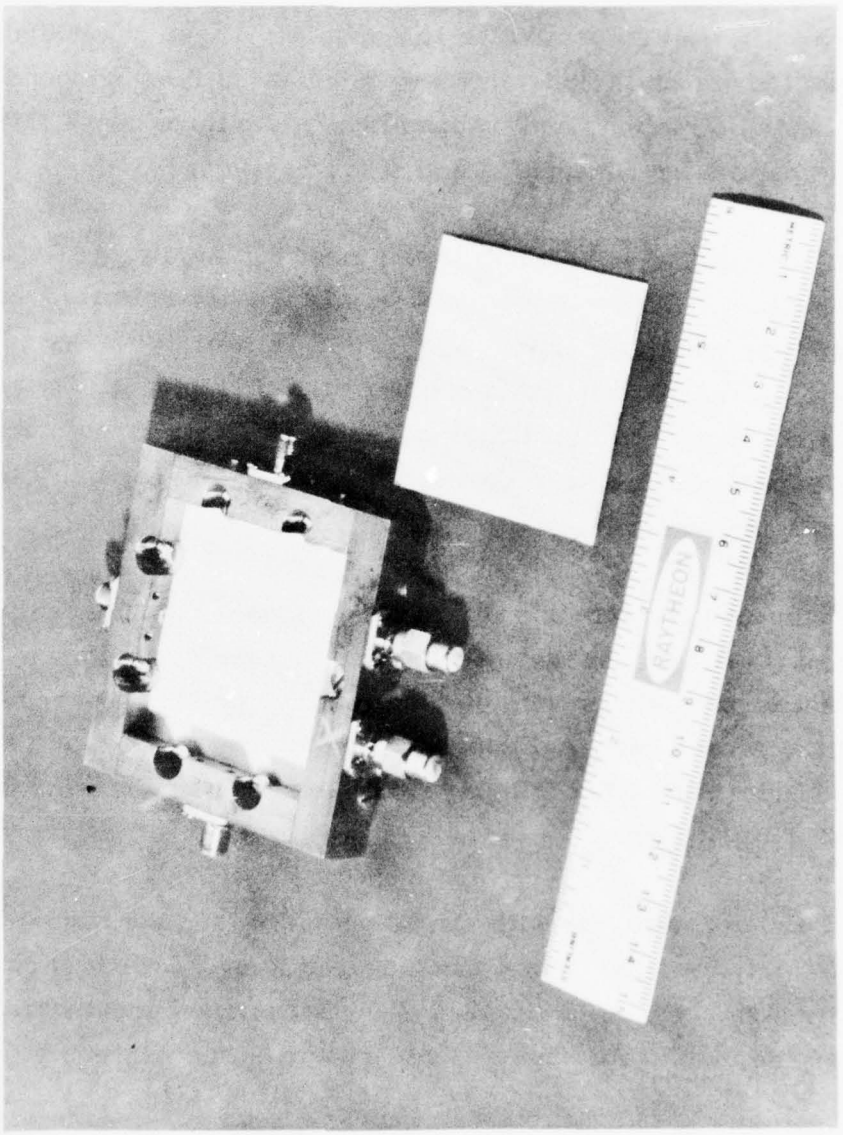

Figure 3-15 Two-Port Gysel Hybrid Realized in TIM-Line Configuration. Terminations are mounted external to the circuit, and can be high-power OSM loads.

3.2.2.3.2.2 Transmission line types

The nonresonant power-combining circuits can be realized in any one of several different transmission line media. Those considered for use in the present program include ordinary microstrip line, suspended microstrip line, balanced stripline, and trapped inverted microstrip (TIM) line. Each has some particular advantages and disadvantages.

Conventional microstrip is the most commonly used of the transmission line types. There is a great deal of experience in its use, and fabrication costs are relatively low. The circuit is accessible for adjustment after fabrication. Microstrip has a number of disadvantages: losses are the highest of any of the types of line; fringing fields are fairly strong, making a high level of isolation difficult to obtain; and techniques normally used for tuning the circuit are inconvenient.

Suspended microstrip offers lower losses than conventional microstrip, and the air gap between the circuit and the ground plane permits convenient tuning, either with dielectric slugs or tuning screws inserted through the ground plane. Fabrication costs are similar to those of conventional microstrip, but fringing fields are greater, making good isolation more difficult to obtain.

Balanced stripline with air dielectric offers the lowest loss and highest isolation of any of the transmission lines. Fabrication costs are relatively high because two ground plane structures are required. The access to the circuit for tuning is difficult once the assembly has been completed.

Trapped inverted microstrip (TIM) line, recently described by Buntschuh,[6] appears to offer a number of advantages for the present program. Figure 3-16 shows the TIM line structure. This is basically a trough line with a dielectric overlay. Compared with conventional microstrip, dielectric losses are reduced because most of the wave energy propagates

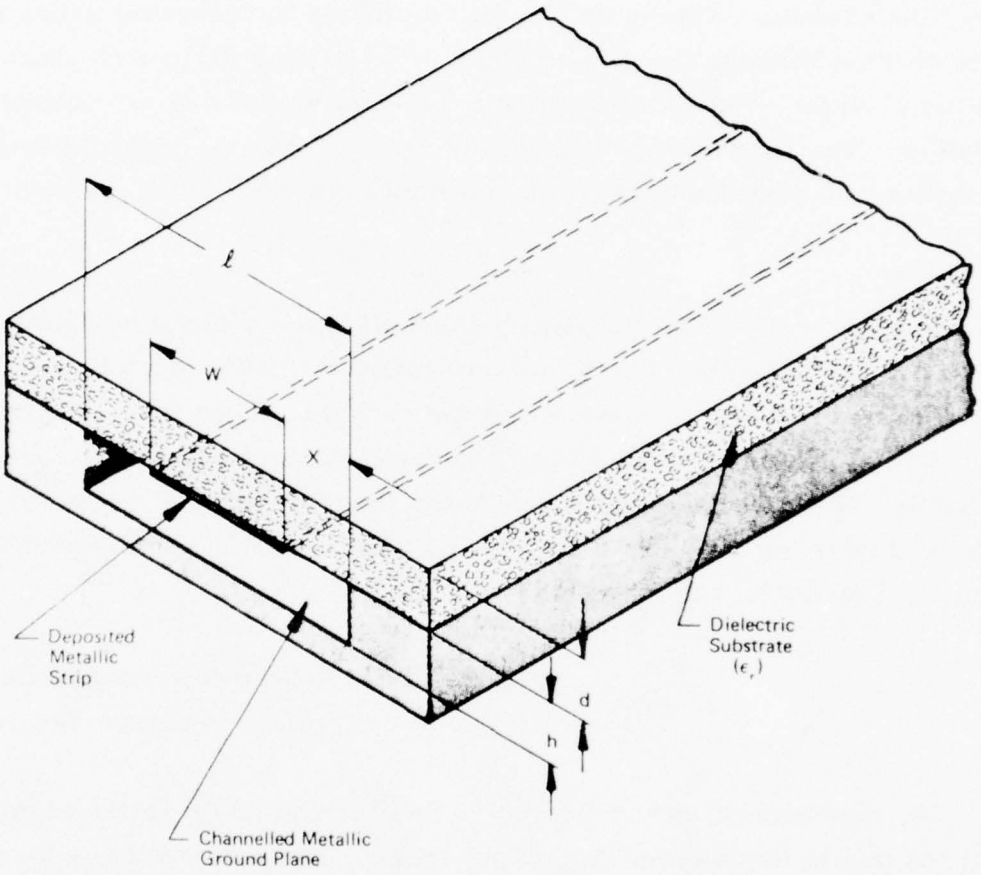

Figure 3-16 Trapped Inverted Microstrip (TIM) Line Structure

in the air gap. Conductor losses are reduced because line widths are greater at a given impedance level, thus reducing current density. Isolation is improved because fringing fields tend to be confined within the dielectric overlay near the channel. Tuning can be accomplished by inserting tuning screws into the channel through the ground plane or by sliding dielectric slugs along inside the channel. Fabrication costs are higher than those for conventional microstrip. The substrate processing is similar, but the ground plane is more difficult to produce because the channel must be formed under the circuit.

Results reported by Buntschuh show effective dielectric constants of about 3 - 3.5 for TIM lines using alumina substrates, which confirms that much of the wave energy propagates in the channel. Loss per wavelength is about 0.05 dB, approximately 60 to 70 percent of that present in conventional microstrip. Much of this loss is conductor loss. A further reduction could be achieved by using a Cr-Cu-Au metallization instead of the simpler Cr-Au system used in Buntschuh's tests.

3.2.2.3.2.3 Progress in nonresonant power-combiner development

The nonresonant power combiner has been pursued as the primary circuit for use in the transmitter output stage. The dielectrically loaded cavity described earlier is at present considered an alternative to be used if difficulties are encountered with the nonresonant power combiner.

The first major steps in the nonresonant power combiner development were the selection of the Gysel-type circuit just described, and the selection of TIM-line as the transmission line medium for use in this circuit. The option of using either a single Gysel circuit with four diode ports or a cascade of units with two diode ports remained at the end of the reporting period.

The two-port and four-port Gysel circuits were extensively

analyzed. Figure 3-17 shows the circuit model used in this analysis. All the transmission line segments Z_1, Z_2, Z_3, Z_4 are $\lambda/4$ long. For convenience, the input, the output, and the termination impedance have been set equal to Z_0, nominally 50 ohms. With this choice of impedances, the input and output ports will be matched if $Z_2 = Z_1\sqrt{N}$ and $Z_3 = Z_0$ for arbitrary Z_1 and Z_4. The choice of the impedances within these constraints will affect the frequency dependence of the circuit. In the analysis, transmission line losses were neglected, but losses caused by mismatches and by dissipation in the internal terminations were included.

Figures 3-18 and 3-19 summarize the computed performance for a two-port 5-GHz Gysel circuit with line impedances $Z_1 = Z_3 = Z_4 = 50\Omega$, and $Z_2 = 70.7\Omega$. In an 18 percent bandwidth centered on 5 GHz, maximum input VSWR is 1.2, maximum output VSWR is 1.1, maximum loss is 0.2 dB, and minimum isolation between outputs is 25 dB.

Figures 3-20 through 3-23 summarize the computed performance for a four-port 5-GHz Gysel circuit. Results for three different cases are shown: (1) $Z_1 = Z_3 = Z_4 = 50\Omega$, $Z_2 = 100\Omega$: (2) $Z_1 = 25\Omega$, $Z_2 = Z_3 = Z_4 = 50\Omega$: and (3) $Z_1 = Z_3 = 50\Omega$, $Z_2 = 100\Omega$, $Z_4 = 25\Omega$. The best overall performance was found in the first case. There, for a 25 percent bandwidth centered on 5 GHz, maximum input VSWR was 1.2, macimum output VSWR was 1.1, maximum loss was 0.2 dB, and minimum isolation between output ports was 30 dB. Case (3) offered lower loss and a better input match, but had poorer isolation and output match.

The computed performance for the Gysel circuits exceeds the requirements on loss, isolation, and bandwidth in the transmitter output stage. In practice, limitations on VSWR will probably be defined by the coax to TIM-line transitions used to make connections to the external microwave system. If losses in the transmission line do not add to the computed losses substantially, a circuit efficiency above 70 percent should be possible.

Symmetry of the power-combiner circuit is important both to insure

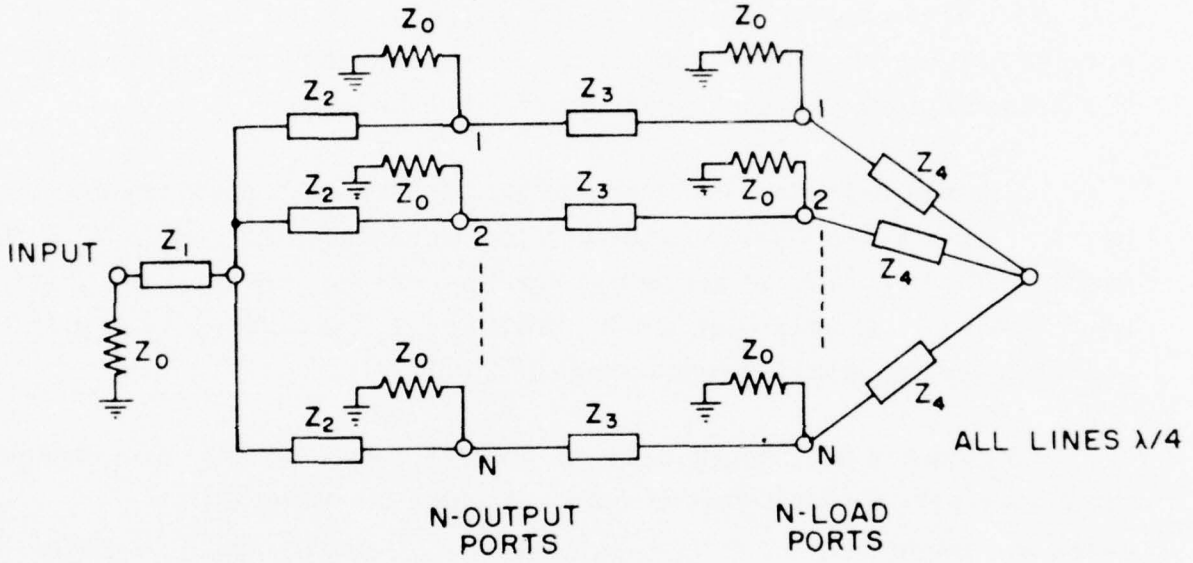

Figure 3-17 Model for a Generalized N-Port Gysel Circuit.

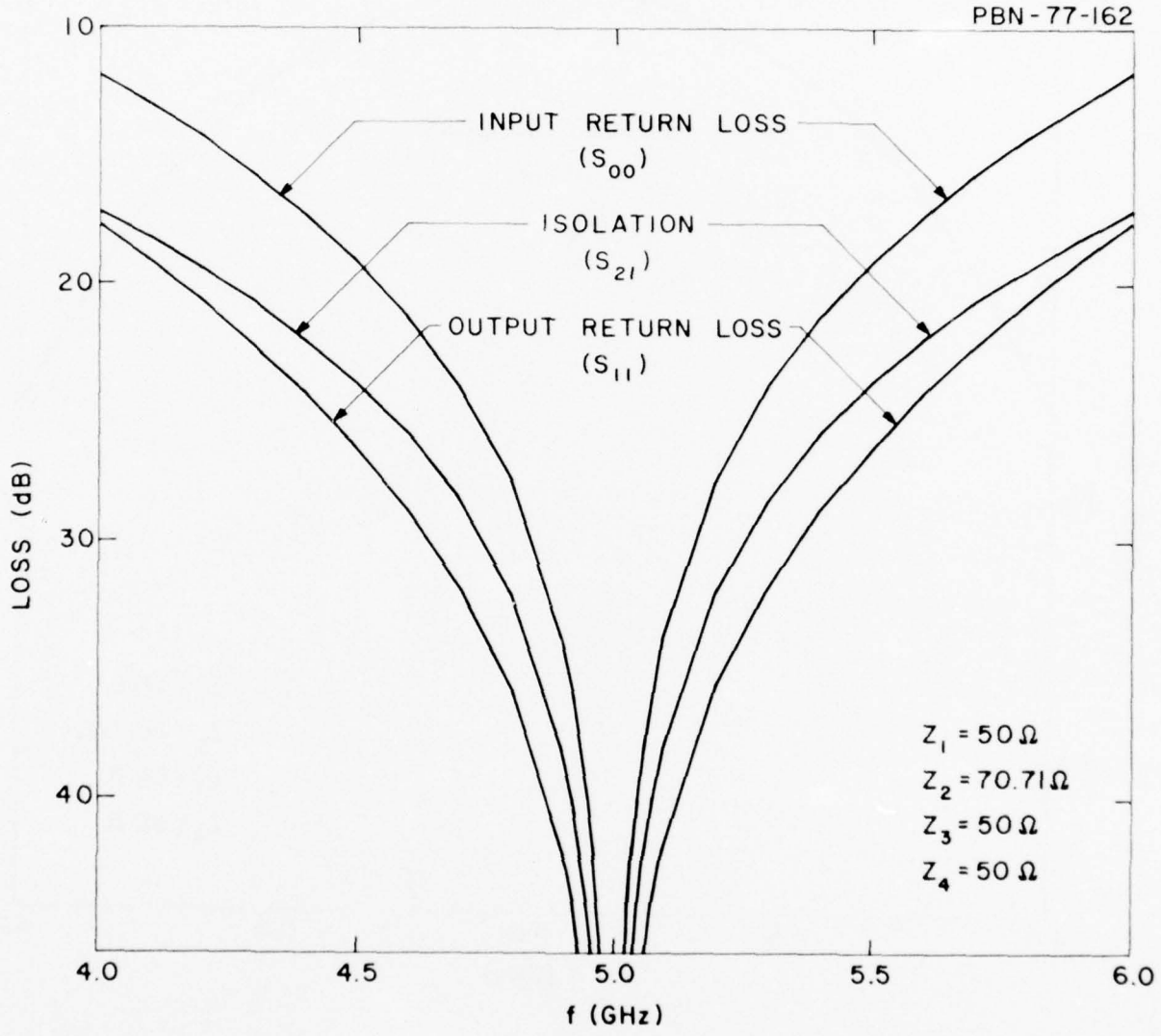

Figure 3-18 Composite Plot Showing Computed Input Return Loss, Output Return Loss, and Isolation between Outputs for a Two-Port Gysel Hybrid.

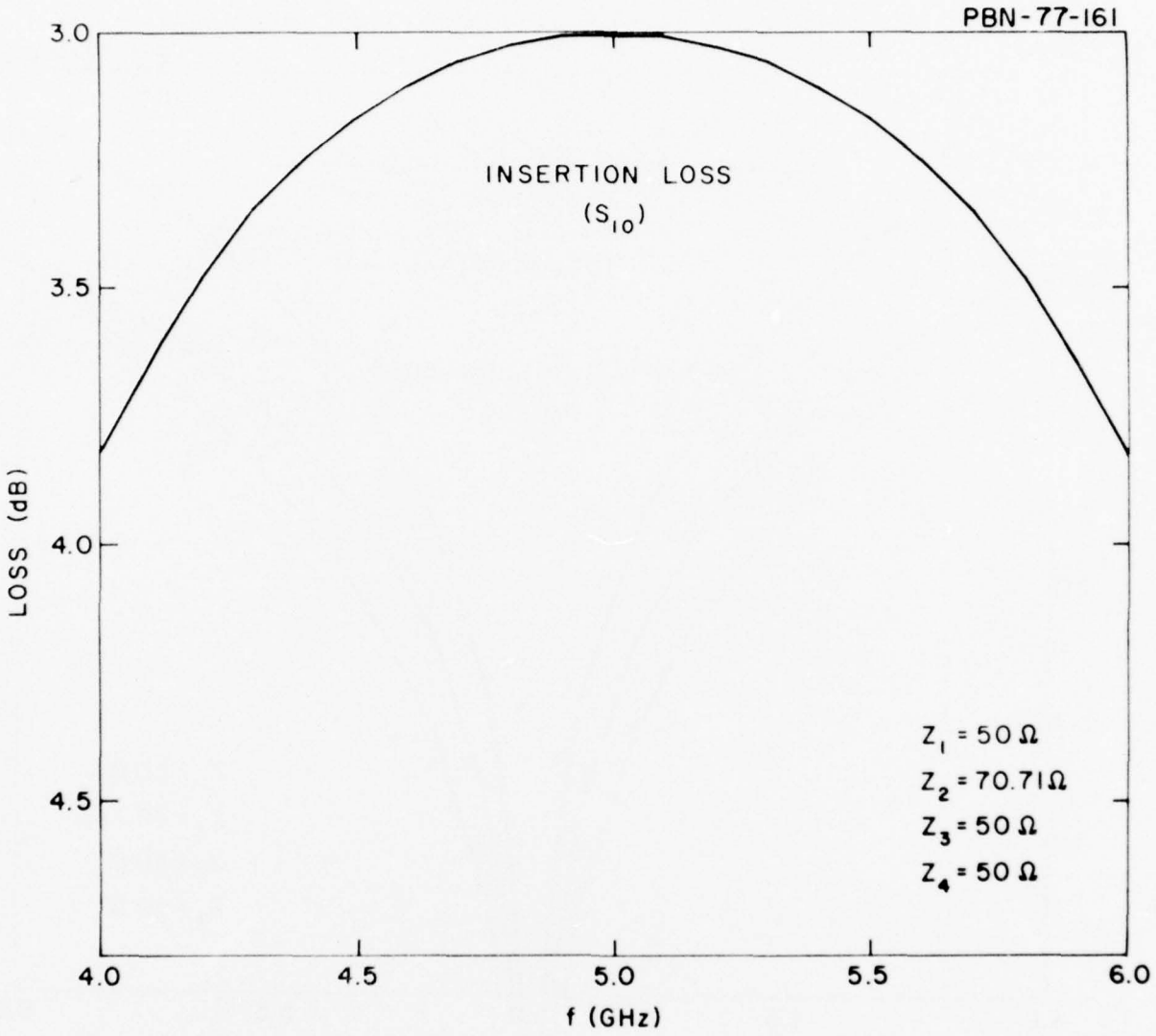

Figure 3-19 Computed Loss from the Common Port to One Diode Port of a Two-Port Gysel Circuit. The nominal power division results in 3 dB loss; loss above 3 dB represents unrecoverable dissipated power.

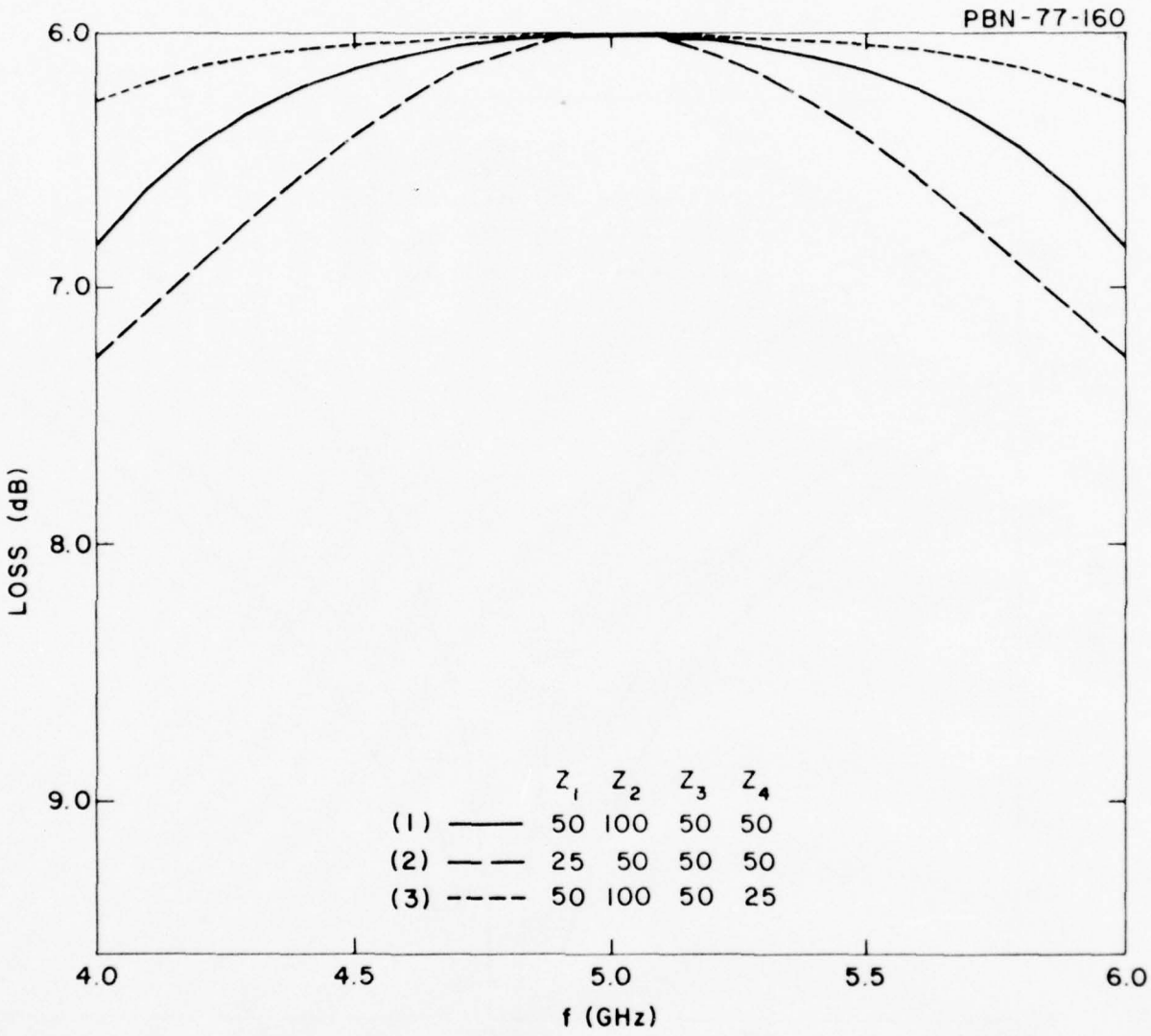

Figure 3-20 Computed Loss from the Common Port to One Diode Port of a Four-Port Gysel Circuit for Three Different Sets of Internal Line Impedances. The nominal power division results in 6 dB loss; loss above 6 dB represents unrecoverable dissipated power.

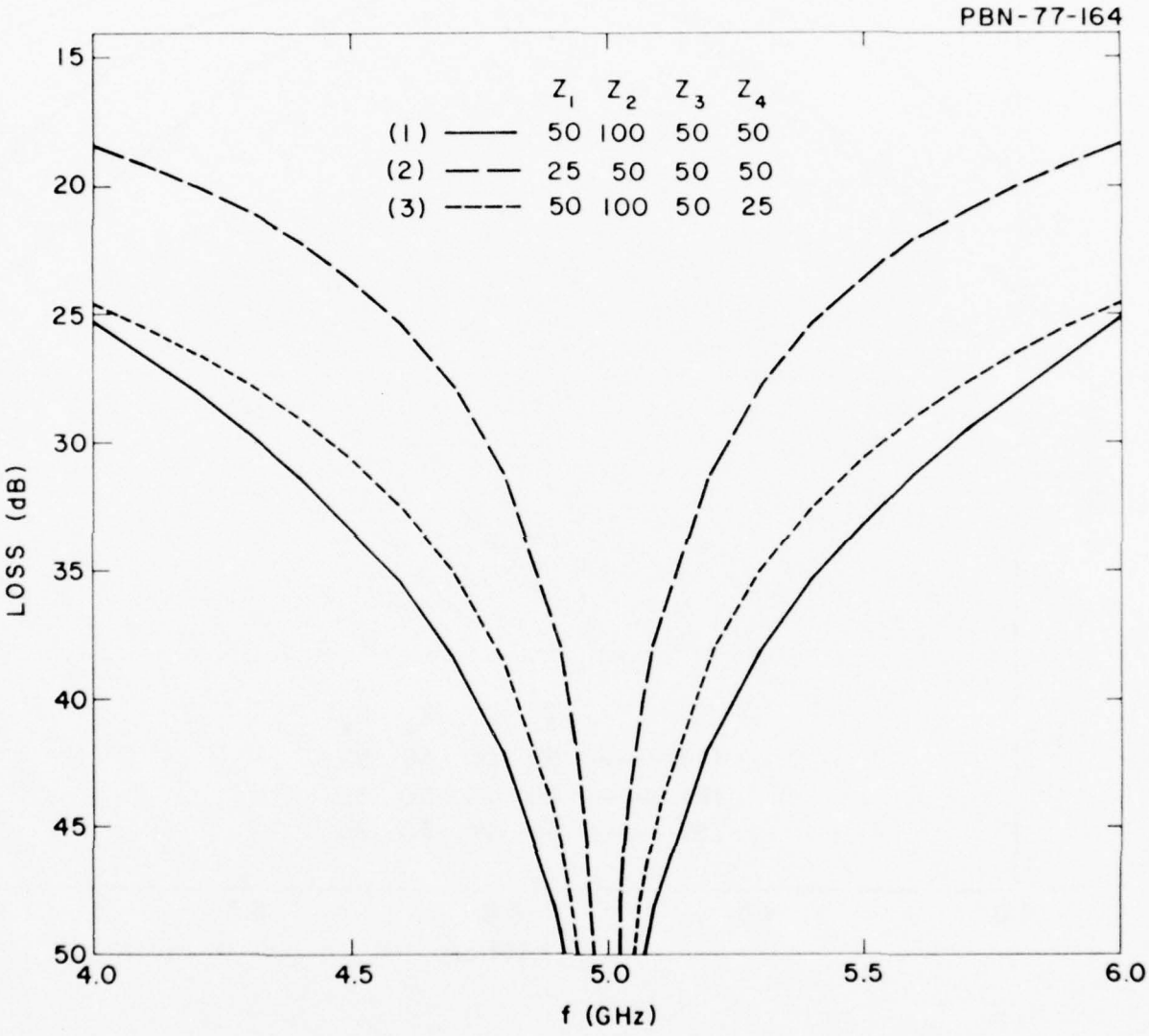

Figure 3-21 Computed Isolation between Two Diode Ports in a Four-Port Gysel Circuit for Three Different Sets of Internal Impedances.

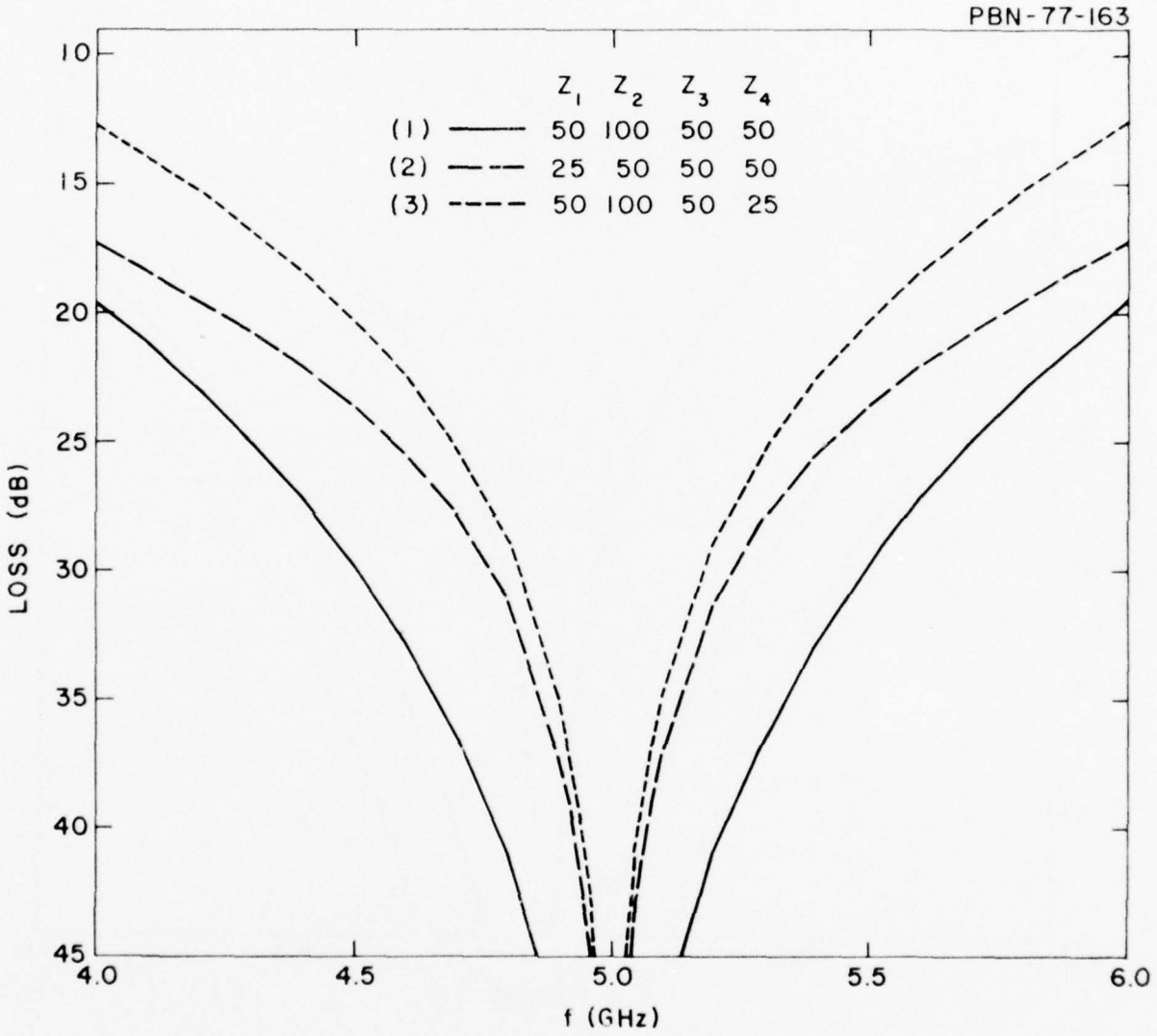

Figure 3-22 Computed Return Loss at One Diode Port in a Four-Port Gysel Circuit for Three Different Sets of Internal Impedances

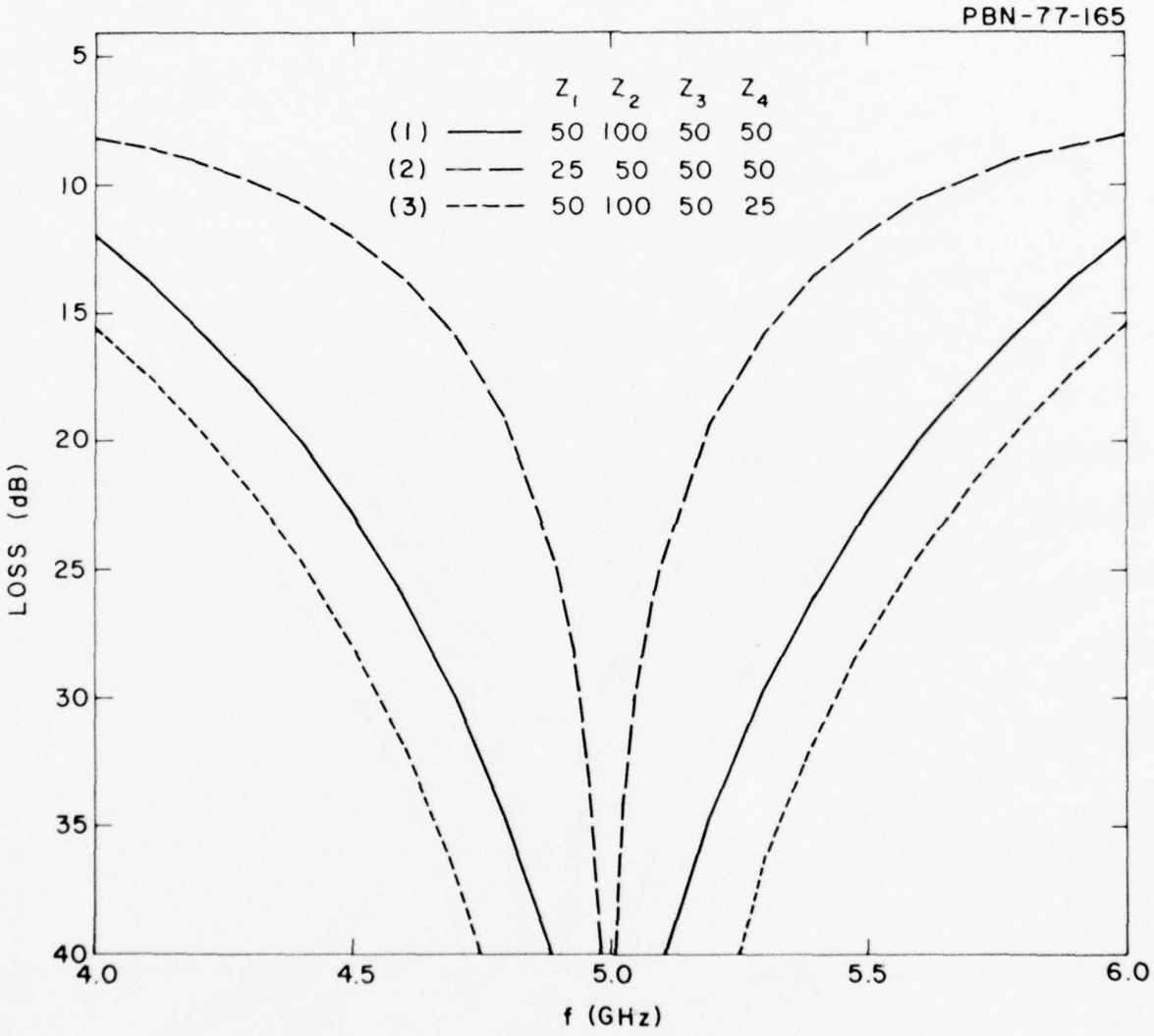

Figure 3-23 Computed Return Loss at the Common Port of a Four-Port Gysel Circuit for Three Different Sets of Internal Impedances.

balance between the signals at the output ports and to reduce the probability of exciting undesired modes in the structure. One problem is that a symmetrical arrangement of the circuit of Fig. 3-17 (i.e., one in which the output ports are indistinguishable) cannot be realized on a plane surface when there are more than two output ports. However, symmetrical circuit topologies are possible with more than two output ports if polyhedral surfaces are used. One possible arrangement for a four-port power combiner is shown schematically in Fig. 3-24. Here, the circuit is spread on the surfaces of a cube. Symmetry is preserved in that the four output ports, to which diode modules are connected, cannot be distinguished from each other without artificially marking the cube. The structure is compact since each TIM-line segment is of order $\lambda/4$ in length. However, bending the TIM-line circuit around the corners of the cube will pose a difficult fabrication problem. It may prove simpler to use a cascade of two-port circuits to obtain the required four diode ports. The performance of the cascaded circuits will not be as good in terms of loss or bandwidth as that of the single four-port circuit, but a circuit efficiency of 70 percent should still be possible.

The hardware for the TIM-line nonresonant power combiner was to be developed in a series of steps. First, 50-ohm line segments of various lengths were to be fabricated and tested, both to gain experience with what was to us a new transmission line medium and to obtain some basic loss and impedance data. A simple two-port Gysel circuit was then to be constructed. Following tests of this unit, the power combiner for the transmitter output stage was to be fabricated. This could be either a single four-port circuit or a two-level cascade of two-port circuits.

At the close of the period covered by this report, ground planes for the 50-ohm TIM line test sections and for the basic two-port power combiner had been completed. The first substrates for the 50-ohm test lines had been received but were rejected for poor-quality metallization. Replacements for these had been received and were awaiting test, after which construction of substrates for the two-port power combiner could proceed. The system shown in Fig. 3-25 had been developed for making transitions between TIM-line and the SMA connectors.

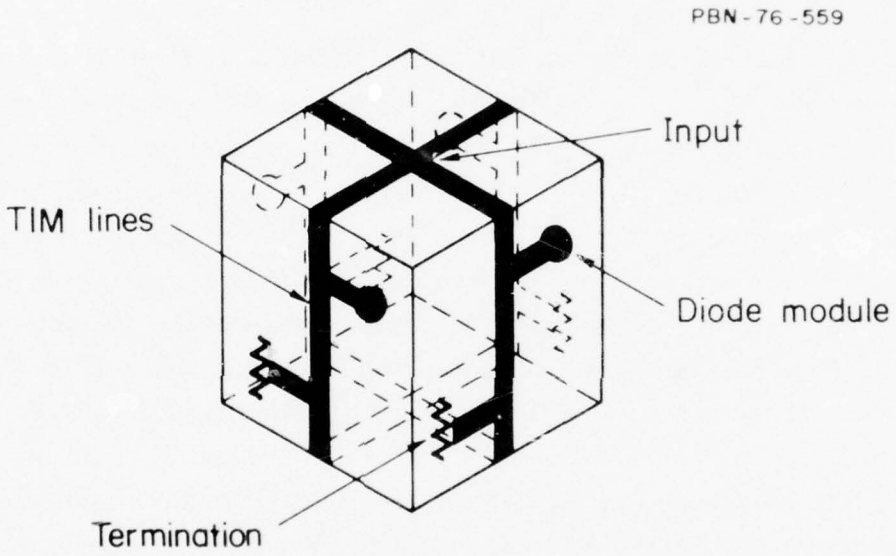

Figure 3-24 Topology for a Symmetrical Gysel Circuit with Four Diode Ports.

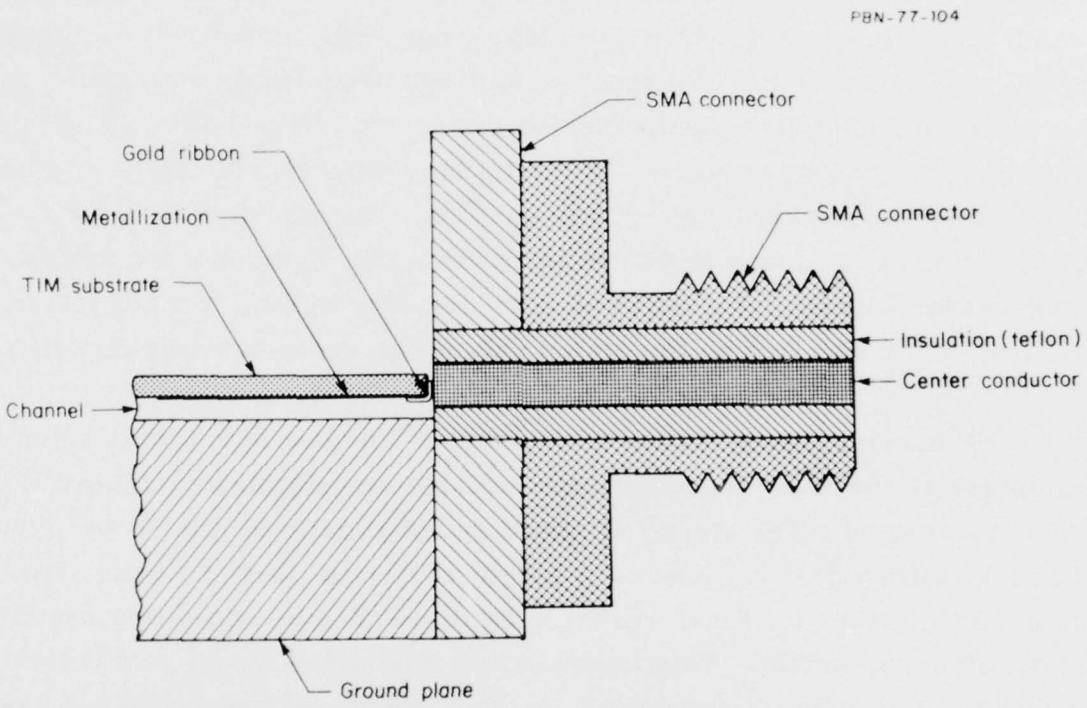

Figure 3-25 TIM Line to SMA Transition. The gold ribbon is thermocompression bonded to the TIM-line circuit metallization, and soldered to the center conductor of the SMA connector using a hot-gas gun.

3.2.3 Diode modules

In the resonant power combiner, the IMPATT diodes are mounted in coaxial line assemblies which are an integral part of the cavity structure. The nonresonant power combiner, in contrast, uses discrete oscillator modules which are coupled to the power-combining network. Eventually, integration of the nonresonant combiner and the oscillator modules as a single structure having a common type of transmission line should be possible. For this reason, TIM-line was selected as the transmission line medium in which to develop the individual high-power oscillator modules for the present program. For convenience in the development work, however, the oscillator modules to be used in the deliverable transmitter will be constructed as separate units rather than integrated with the power-combining circuitry.

For preliminary testing of the IMPATT diodes in a simple circuit analogous to the TIM-line oscillator module, an existing coaxial oscillator circuit was used. The circuit is shown schematically in Fig. 3-26. The diode is mounted at the end of a length of 7-mm 50-ohm line. The single slug serves to transform 50 ohms to the circuit impedance required at the diode terminals. This impedance typically has a real part between 0.6 and 1.0 ohm and a capacitive reactive component between 4 and 8 ohms. A simple computer routine was written which gave the impedance at the diode terminals in terms of the position and dimensions of the slug. Bias was fed to the diode along the coaxial center conductor through a commercially available bias Tee. A coaxial test kit was assembled and calibrated for making power output measurements on the coaxial module.

Tests in the simple coaxial module were intended to provide data on the RF impedance required by the diodes for efficient operation. Such data are not easily obtained from the top-hat oscillator normally used for preliminary diode evaluation. The impedance data were to be used in the design of TIM-line oscillator modules.

PBN-74-655

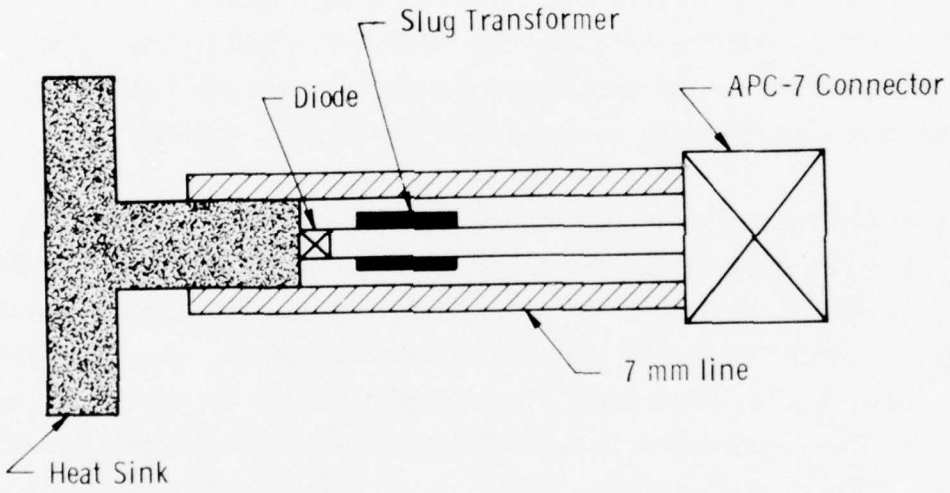

Figure 3-26 Simple Coaxial Oscillator Module

Tests in the simple coaxial module were not successful. Strong bias circuit oscillations were encountered, both with high-power four-mesa diodes and with older small-area single-mesa diodes. The output spectrum of the coaxial oscillator module in the presence of strong bias circuit oscillations is shown in Fig. 3-27. The cause of these bias circuit oscillations was excessively low bias circuit impedance. Shunt capacitance of the bias Tee was about 46 pf – approximately three times larger than the capacitance of the bias choke in the usual top-hat oscillator. Also, the RF circuit placed the 50-ohm line impedance in parallel with the bias circuit, further reducing the effective bias source impedance. In principle, these oscillations could have been eliminated by raising the bias source impedance.[1] This would be accomplished by using a low-capacitance bias Tee and by inserting a low-capacitance DC block in the coaxial center conductor to isolate the module and bias Tee from the remainder of the 50-ohm system.

As an alternative to modifying the coaxial system, single-diode oscillator tests were made in the six-diode cavity circuit fabricated during the previous program.[3] In this circuit, the diodes are mounted in a coaxial environment similar to that of the simple coaxial module. (See Fig. 3-29.) The cavity provides isolation from the external 50-ohm system. The nonresonant bias line termination has smaller shunt capacitance than the bias Tee used with the coaxial module. These differences permitted stable operation of the diodes without bias circuit oscillations. Diodes from lots 907, 909, and 910 were tested in the cavity circuit, and produced power outputs within 0.5 dB of those obtained in the top-hat oscillator. The cavity circuit can also be used for diode impedance measurements, but such measurements on the new four-mesa devices had not been completed by the end of September 1976.

Lacking precise data on the impedance of the new four-mesa diodes, we decided to proceed with a preliminary design of the TIM-line oscillator using the impedance previously measured for the smaller (7-mil mesa) four-mesa diodes fabricated during the previous program.[3] This diode impedance, -0.8 + j6 ohms, should be fairly close to that of the new diodes,

PBN-76-447

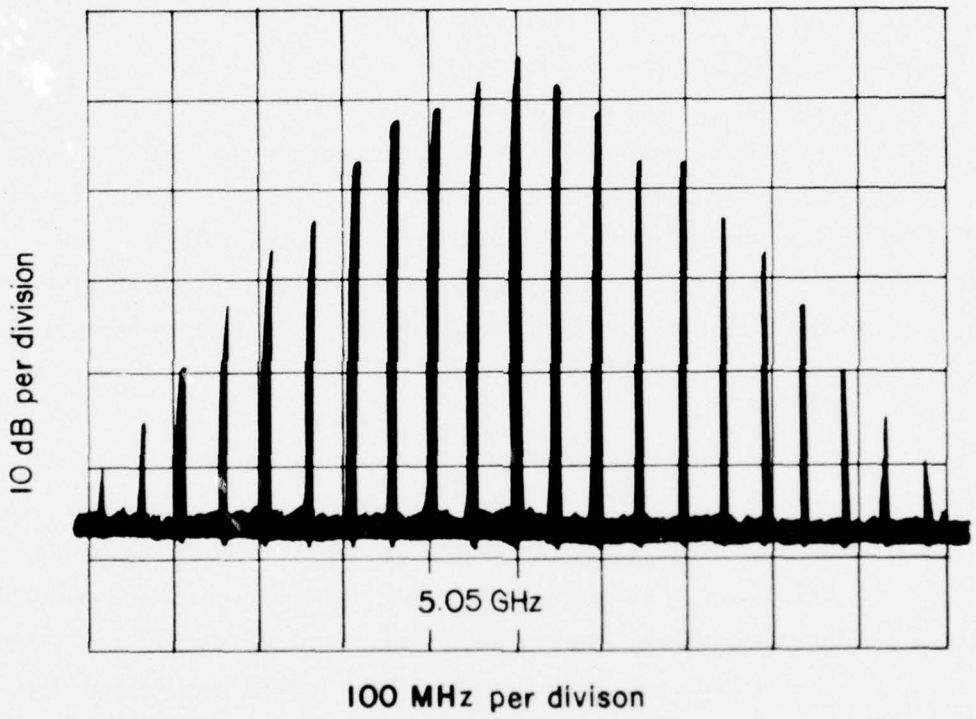

Figure 3-27 Output Spectrum of the C-Band Coaxial Oscillator with Strong 50-MHz Bias Circuit Oscillations.

and the circuit design process should reveal potential problem areas. Refinement to accommodate slightly different diode impedances can be made later.

The advantages of the TIM-line in terms of low loss and reduced fringing field have been described previously. One shortcoming which becomes evident when designing the oscillator module is the difficulty of fabricating low-impedance TIM-lines in a well-controlled fashion. This is shown in Fig. 3-28, which gives impedance as a function of line width for different channel widths. For impedances below ~20 ohms, the characteristic impedance Z_o of the line becomes a very rapidly varying function of line width. This occurs when the line width approaches the channel width, leaving only a small gap between the printed conductor and the side walls of the channel. Maintaining a particular (low) impedance requires a high degree of precision, both in the line and channel widths and in the alignment between the dielectric substrate and the ground plane.

Figure 3-29 shows the difficulty which arises when one tries to design a single-step $\lambda/4$ transformer to match the diode impedance to a 50-ohm line. Also given are two alternative transformer designs which should require less precision in substrate alignment and dimensional control of the conductors. The single-section transformer requires use of a 198-mil-wide line with a 200-mil-wide channel. Besides the obvious problem of extremely tight mechanical tolerances in such a structure, one will also encounter excessive losses, and possibly electrical breakdown, because of the high electric field in the narrow gap between the microstrip conductor and the channel wall. The three-section transformer accomplishes the desired matching to the diode impedance without requiring any line impedance lower than 25 ohms. The overall bandwidth of the three-section transformer can be made greater than that of the single-section transformer, and the precision required for the 176-mil-wide lines will certainly be less. Some price is paid in overall size, however. The series capacitive gap, followed by a length of 50-ohm line, is in many ways the most attractive matching network. Only 50-ohm lines need be printed, and the capacitive gap provides DC isolation from the remainder of the

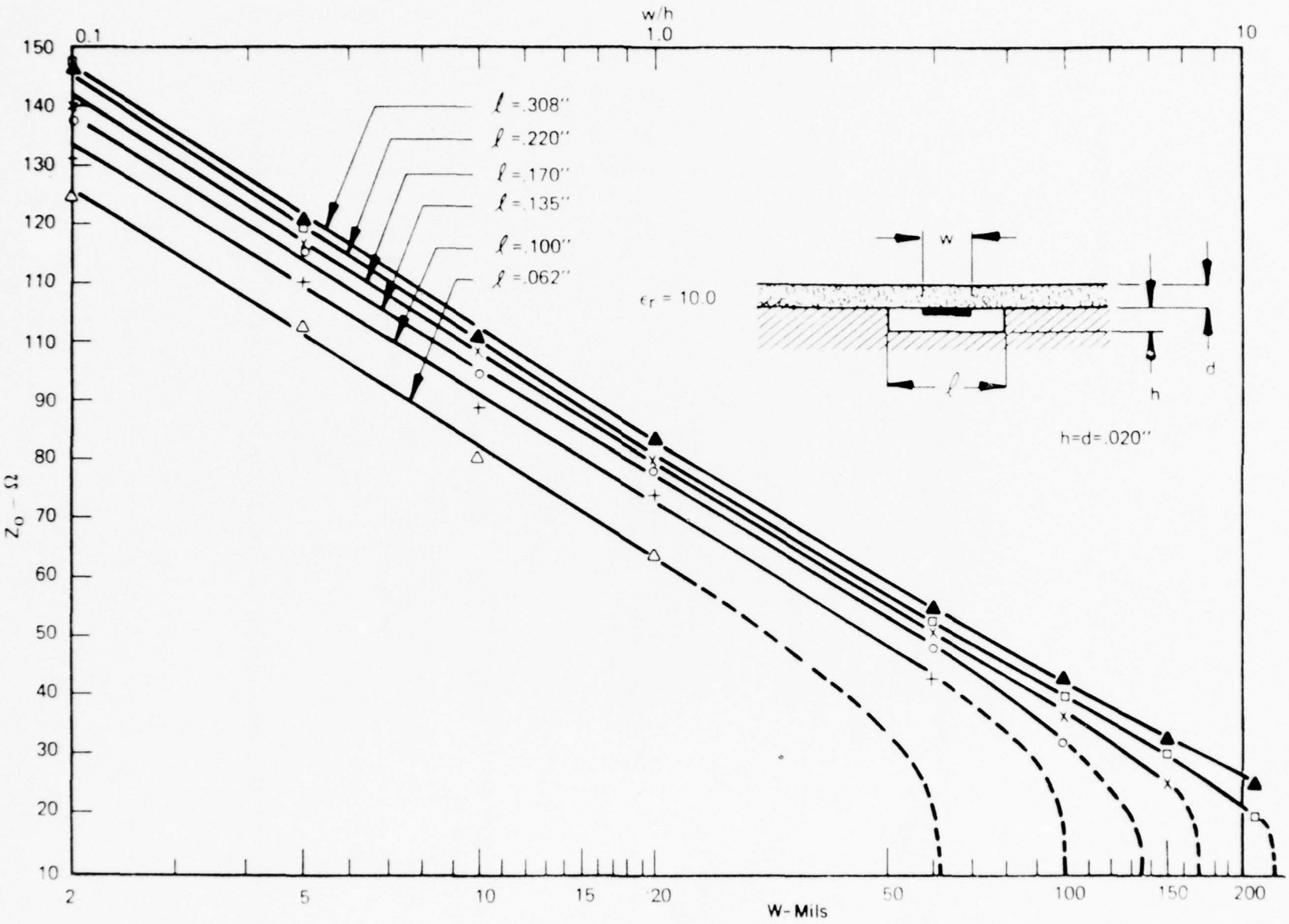

Figure 3-28 TIM Line Impedance as a Function of Line Width for Several Different Channel Widths. A channel depth of 20 mils has been assumed.

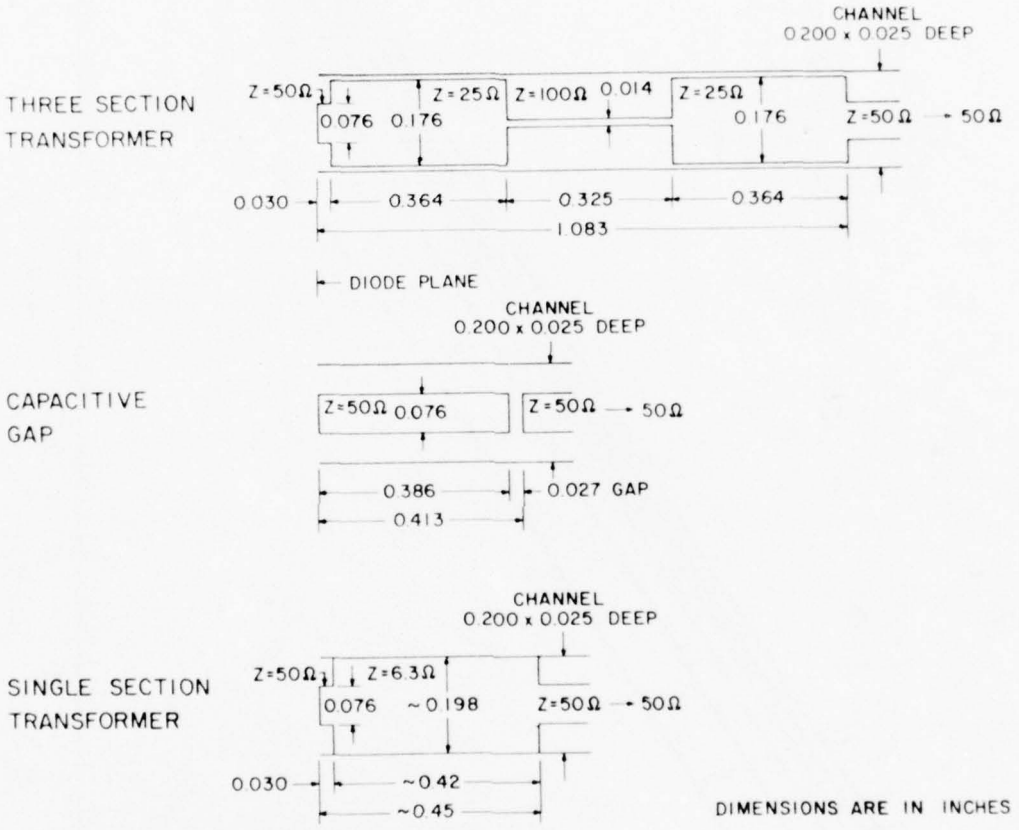

Figure 3-29 TIM-Line Circuits to Transform 50 Ohms to 0.8 + j6.0 Ohms.

microstrip circuit. This isolation is important, because the diodes which will be connected to the ends of the 50-ohm stub lines must be independently biased. Further, the capacitance of the gap is so small that it prevents the external RF circuit from having any appreciable loading effect which would lower the bias circuit impedance. This helps to promote stability against bias circuit oscillations.

While all of the circuits shown in Fig. 3-29 can provide the required impedance at the diode terminals, none has any provision for tuning after fabrication. The capacitive gap circuit can be tuned by adding variable shunt capacitances spaced a finite distance on either side of the gap. Such shunt capacitances can be realized with tuning screws inserted into the channel through the ground plane, or with variable stub lines realized by sliding dielectric slugs in the stub-line channel.

Figure 3-30 shows the impedance range which can be obtained at the diode terminals by adjusting the shunt capacitors in a "series-gap" oscillator circuit operating at 5 GHz. The nominal center of the impedance range is 0.8-j6 ohms, the circuit impedance required by typical high-power diodes developed during the previous program. The circuit model used for obtaining the impedance values is also shown in the figure. For this preliminary analysis, line lengths appropriate to a relative dielectric constant of unity were used. Note that nearly independent adjustment of the real and imaginary parts of Z is possible, with C_2 controlling Im [Z] and C_1 controlling Re [Z].

At the end of September 1976, the capacitive gap circuit with shunt-tuning capacitors had been selected for use as the oscillator module. Final RF circuit design was awaiting data from terminal impedance measurements of the new four-mesa diodes. The bias decoupling network also had to be designed before fabrication of the module could be started.

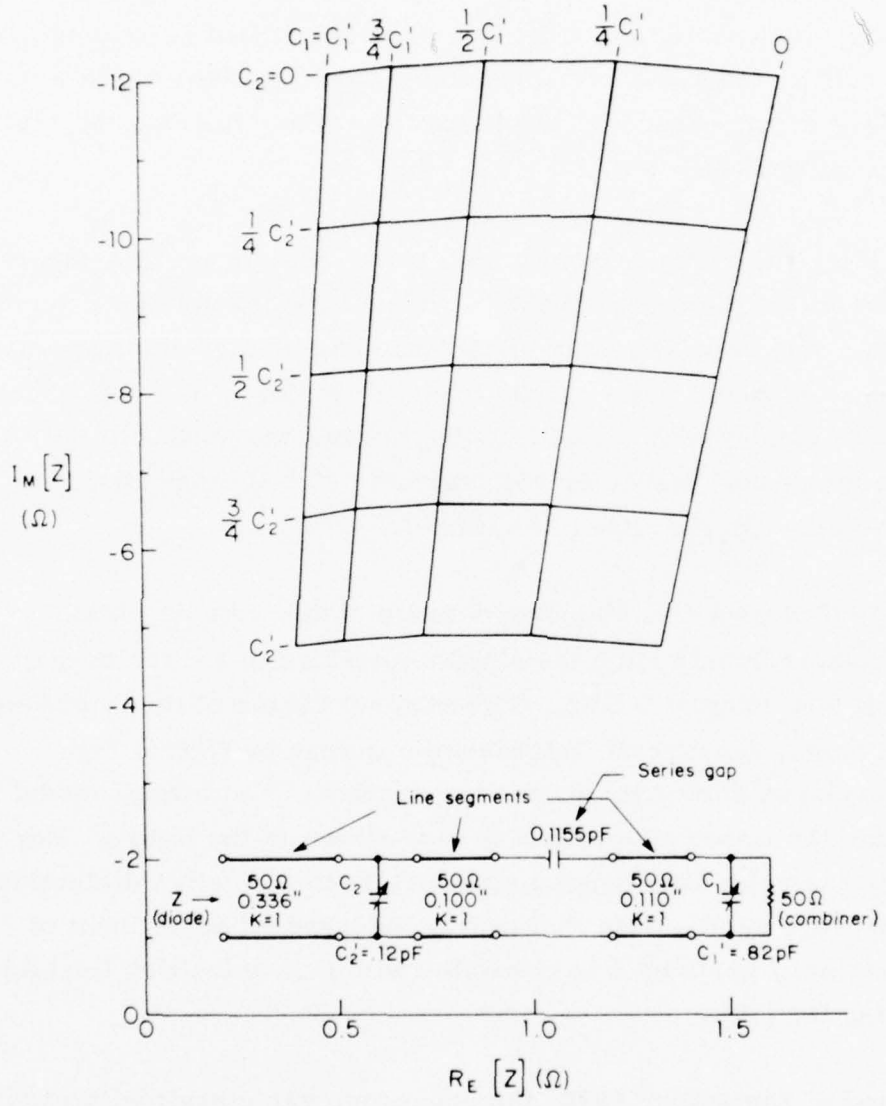

Figure 3-30 Impedance Presented to the Diode Terminals in a Series Gap TIM-Line Oscillator Circuit Having Shunt Capacitors for Tuning.

3.3 Multichannel Current Regulator

3.3.1 General bias circuit considerations

For bias voltages less than the breakdown voltage V_B, a reverse-biased IMPATT diode draws essentially no current. The current is a rapidly increasing function of voltage for bias voltages larger than the breakdown voltage. With this type of voltage-current characteristic, the operating point of the diode can be most smoothly controlled if bias is supplied from a current-regulated source.

The voltage-current characteristic of a high-efficiency GaAs Read IMPATT diode is quite different in the oscillating and nonoscillating states. Self-rectification of the large RF voltage across the diode tends to depress the DC operating voltage in the oscillating state. This depression may be sufficient to cause regions of incremental negative resistance to appear in the DC voltage-current characteristic of the diode. This behavior is illustrated in the curve tracer data of Fig. 3-31. The negative resistance may produce oscillations in the bias circuit.

Brackett[1] has given a good phenomenological explanation of the origin of the negative resistance and of the techniques required to stabilize the bias circuit. Basically, the bias circuit is stabilized by maintaining a bias source impedance that is sufficiently large to make the net bias circuit resistance (source plus load) positive under all operating conditions. Because the negative resistance may extend to frequencies above 100 MHz, stability can be assured only if the bias source impedance is kept large for frequencies well into this region. This usually requires a combination of active and passive circuit techniques.

The voltage-current characteristic of an IMPATT diode typical of those to be used in the transmitter output stage is shown in Fig. 3-32. It was recorded under oscillating conditions. The voltage under non-oscillating conditions at the normal operating current of ~600 mA is

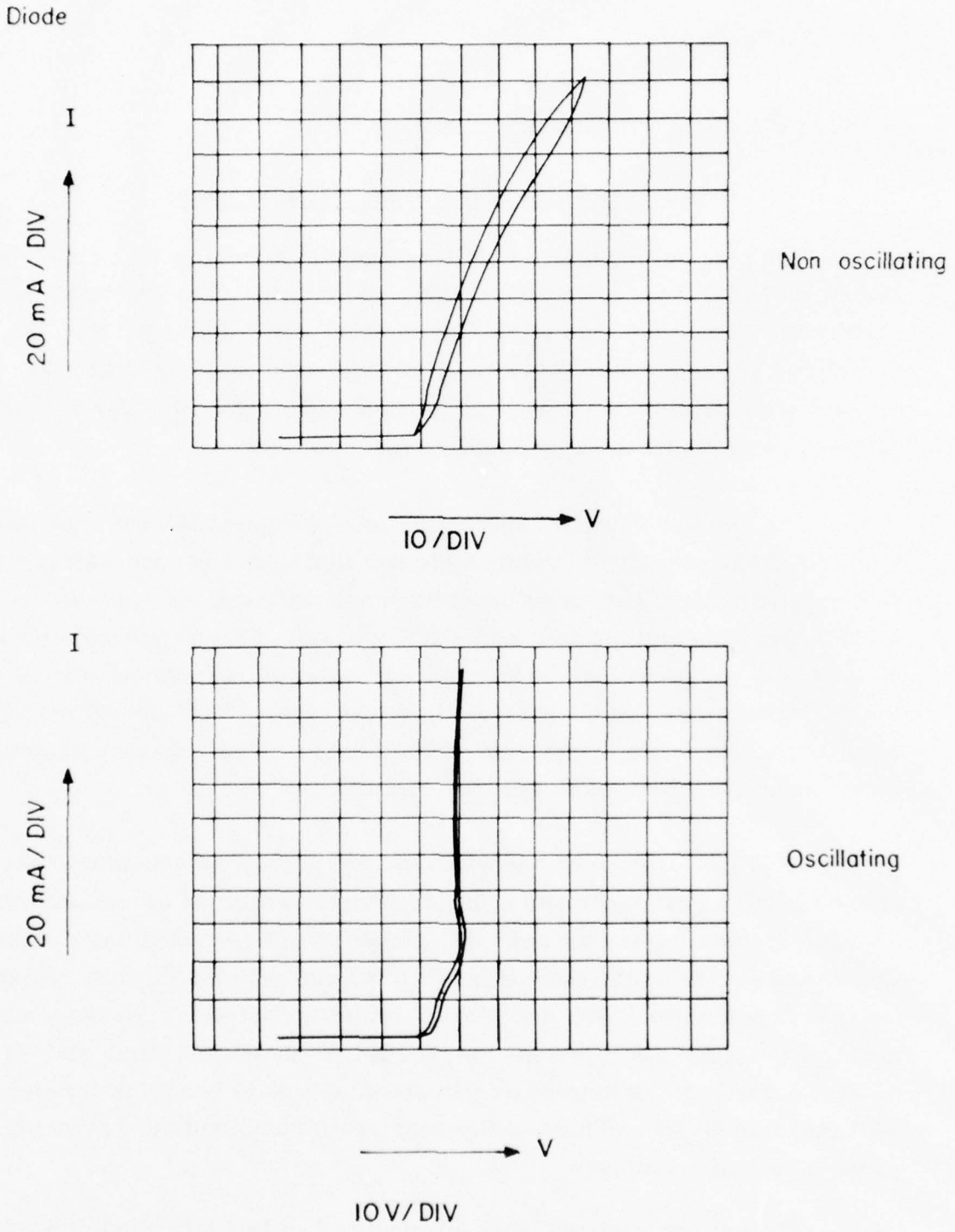

Figure 3-31 V-I Characteristics of a GaAs Read Diode under Oscillating and Nonoscillating Conditions.

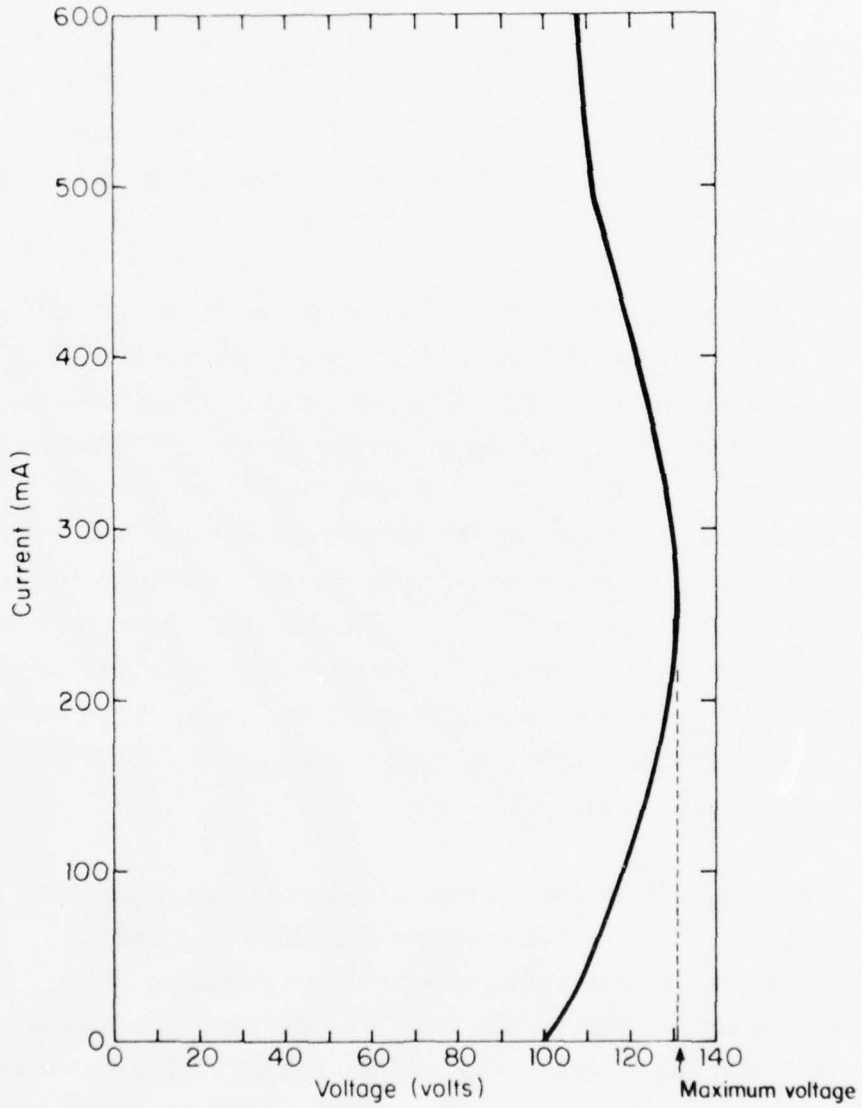

Figure 3-32 Voltage-Current Characteristic, Recorded under Oscillating Conditions, of a High-Power GaAs Read IMPATT Diode Typical of Those To Be Used in the Deliverable Transmitter.

is 60 to 70 V higher than that plotted. Such a voltage produces a power dissipation which quickly causes diode failure. Consequently, operation at maximum current in the nonoscillating mode must be avoided.

The operating voltage under oscillating conditions is a strong function of the RF load impedance. Some tuning conditions may produce an operating voltage smaller than the room-temperature breakdown voltage. We can use this variation of voltage with load impedance to determine if we have achieved correct tuning of the diode.

While the voltage-current characteristic of the oscillating Read diode may imply some stability problems, it has one feature which is of benefit in the present transmitter design. The total voltage excursion between the initial flow of current at V_B and the operating current (500-600 mA in Fig. 3-32) is much smaller in the oscillating state than it would be in the nonoscillating state. By choosing the injection-locked oscillator mode for the transmitter output stage, we guarantee that the diodes will always be in the oscillating state. Since the nonoscillating state never has to be accommodated, a current regulator with smaller voltage compliance, operating from a lower-voltage primary power supply, can be used. With less voltage drop across the regulator, it will dissipate less power, and the overall system efficiency will be higher.

In our work with active current regulators, we have found that an absolute minimum of 3 to 5 V across the regulator is required if control is to be maintained. Lower voltages result in saturation of the series pass transistors and loss of regulation. For the diode characteristic shown in Fig. 3-32, current control can be maintained through turn-on as the bias current is brought up from zero, provided a primary supply of 133 to 135 V is used. This is within the range of adjustment of the DC-to-DC inverter tentatively selected for the transmitter (Sec. 3.4). The voltage drop across the regulator will then be 20 to 25 V at the nominal operating current. For reasons of overall efficiency, it may be preferable to reduce

this voltage drop by choosing diodes or tuning conditions having a smaller maximum voltage-to-operating-voltage ratio. This possibility will be investigated during final development of the transmitter output stage.

3.3.2 Bias requirements

The transmitter design originally proposed used five diodes in the output stage. Each was to be capable of 10.7-W CW output with 23 percent efficiency at 5 GHz. When combined in a circuit having 70 percent efficiency, these diodes would produce 40-W output. Each of the five diodes would require 465 mA of bias current at the 100 V (nominal) operating voltage, and total power consumption in the output stage would be 232 W. The current regulator feeding the output stage would require five outputs capable of at least 465 mA.

Since diodes having at least 15-W CW output are now available, present plans call for a four-diode output stage. Averaging results from several diode lots operating at 5 GHz, one finds that 15 W with 26.5 percent efficiency can be produced with 540 mA of bias current and an operating voltage of 105 V. The requirements for the 40-W output stage are now:

Devices: four diodes, 14.7-W CW each
Bias: 105 V, 528 mA each diode

Total Power Consumption: 215 W.

The lower power consumption of the new design will recover some of the power budget overrun which occurred in the VCO-driver subassembly, and keep the overall transmitter power consumption close to that originally proposed.

3.3.3 Current regulator circuit

A multichannel current regulator circuit suitable for use with the older 10-W diodes was described in the Technical Proposal for this program. When initial tests of the new, large-area diodes showed that operating currents of 750 mA or more were sometimes required for maximum power output, it was thought that substantial redesign of that regulator would be required. The original circuit had a 600-mA-per-channel limit on output current. Later tests showed that 15-W output at 5 GHz was typically achieved with 500 to 570 mA of bias current, which was within the capabilities of the original design.

Figure 3-33 shows a four-channel version of the original regulator circuit which is now to be used in the deliverable transmitter. For simplicity, only two of the output channels are shown explicitly. Component values are listed in Table 3-6. Each of the four outputs is capable of delivering up to 600 mA. The output channels are driven by a single master control unit containing the integrated circuit 1C-1. Adjusting the resistor R_1 changes the currents of all outputs simultaneously. Currents of the individual diodes are adjusted independently around the nominal value by changing the settings of the potentiometers R_9. The protective circuit operating through the zener diodes D_2 shuts down the entire regulator if any one of the IMPATT diodes fails to a short-circuit condition. This should prevent any damage to the regulator and to the remaining IMPATT diodes.

While the circuit of Fig. 3-33 can meet the bias current requirements of the output stage, it is not yet certain that the R_1-L_1 combination will maintain a sufficiently large high-frequency source impedance to prevent bias circuit oscillations. Some circuit modification may be performed during evaluation of the regulator to insure stability. Construction of the circuit is to take place during the second half of the program.

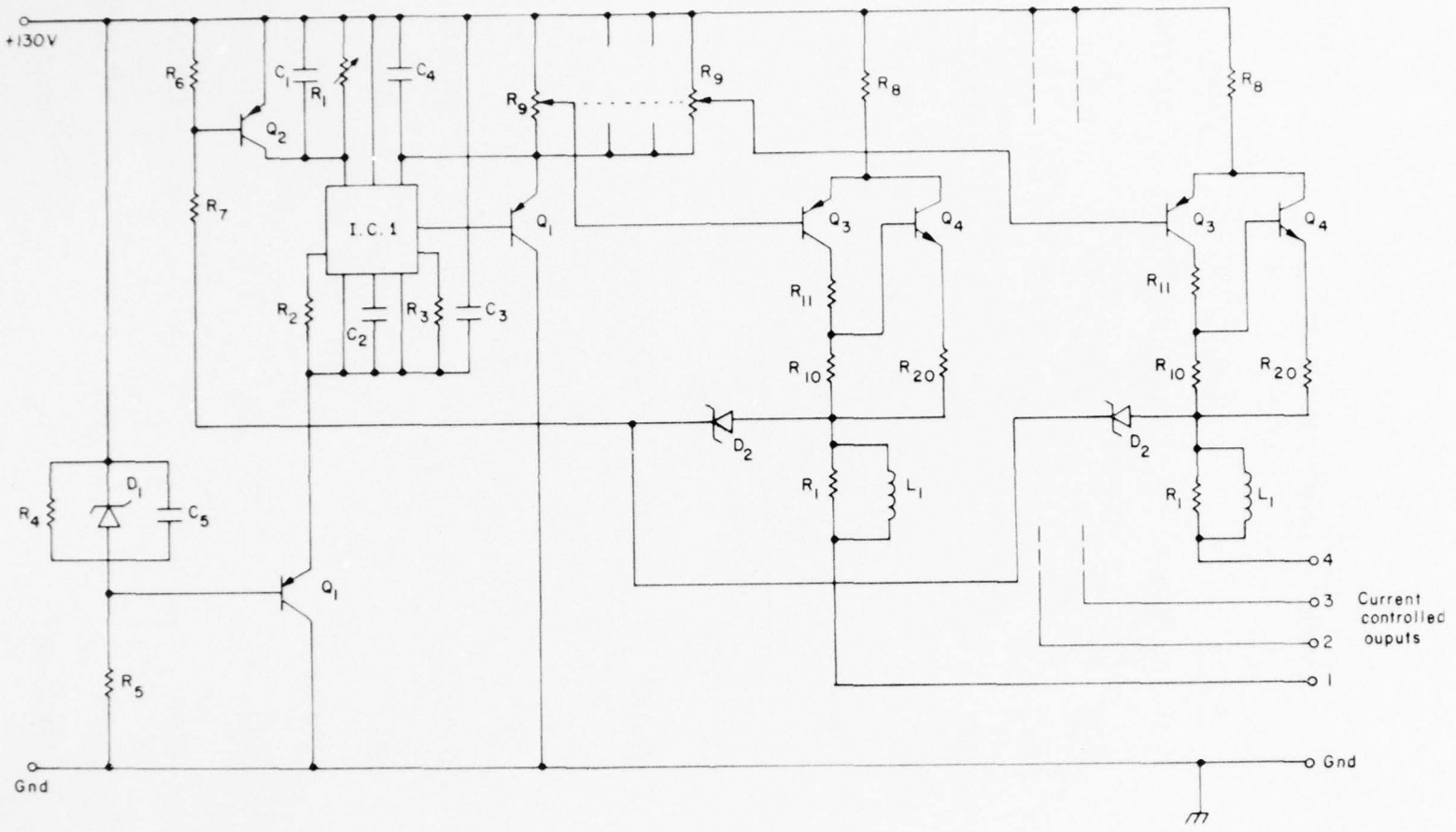

Figure 3-33 Circuit Design for the Multichannel Current Regulator.

TABLE 3-6

TYPICAL PARTS VALUES

Item	Value	Item	Value
R_1	4.7K, or 5K pot	C_1, C_2, C_5, C_6, C_7	.01/ 200 V
R_2	2.4K	C_3, C_4	4.7/ 25 V
R_3	15	C_8	10/ 5 V
R_4, R_5	27K	C_9	510 pF
R_6, R_{19}, R_{25}	1K	C_{10}	20 pF
R_7, R_{13}, R_{14} R_{24}, R_{26}	10K	D_1	1N938
R_8, R_{20}	10/ 1-7 W	D_2	1N4757
R_9	1K pot	D_3, D_4, D_5	1N4004
R_{10}	68	Q_1	2N5415
R_{11}, R_{12}	470	Q_2, Q_6	2N4125
R_{15}	500 pot	Q_3	2N6211, MJE350
R_{16}	47	Q_4	2N6308, MJ410
R_{17}	100K pot	Q_5	PNP-Low voltage
R_{21}	100	Q_7	NPN-High voltage
R_{22}, R_{23}	100K	IC1	LM304
R_{27}	1.5K	IC2	MC1437P
S_1	3POT M.C.	L_1	82μhy
S_2	SPST		

3.4 The DC-to-DC Inverter

The function of the DC-to-DC inverter is to convert the 28-VDC primary power to the 130-V (nominal) level required as an input for the current regulators which drive the IMPATT diodes in the transmitter. Initially, we planned to use a 120-V inverter. However, the voltage-current characteristic of the new large-area IMPATT diodes and the minimum voltage drop allowed across the multichannel current regulator dictated the use of a 130-V unit.

The current regulators in the VCO-driver subassembly were designed to accept 120-V input. The larger inverter output voltage will be accommodated either by readjusting the current regulators or by reducing the applied voltage externally with a zener diode as shown in Fig. 2-1.

The multi-channel current regulator feeding the transmitter output stage and the current regulators in the VCO-driver subassembly consume essentially no current. Consequently, the total current required from the inverter will be approximately equal to that consumed by the IMPATT diodes. This is 350 mA in the driver and 4 x 528 mA, or 2.11 A, in the output stage, giving a total current requirement of 2.46 A. A 2.5-A (nominal) current rating should be sufficient.

At the outset, we recognized that the state-of-the-art for DC-to-DC inverters was such that the size and weight goals for the entire transmitter package would be exceeded by the inverter alone. Power supply development was not considered as one of the primary objectives of this program, and it appeared unlikely that major improvements could be made in the relatively mature power supply technology. Consequently, we decided to purchase a standard commercially available inverter for use in the deliverable breadboard transmitter.

One inverter which appears to meet the needs of the transmitter as presently planned is the Model CEA2-C-130Z-252, manufactured by

CEA Division of Berkleonics, Inc., San Luis Obispo, California. The specifications of this unit are given in Table 3-7. A size reduction from that shown to 6 1/16 x 4 13/16 x 6 13/16 in.^{3} may be possible. Consultation with the manufacturer is planned to confirm this. If the unit achieves 80 percent efficiency at full output, the current drawn from the 28-V supply will be 14.29 A. Added to the .67 A required by the Gunn oscillator in the VCO-driver subassembly, this gives a current drain of 14.96 A for the complete transmitter. This is about 10 percent larger than the current drain originally projected.

At the close of the period covered by this report, plans were to discuss the possible size reduction of the CEA2-C-130Z-252 inverter, and to search for other inverters suitable for use in the transmitter. The results of this investigation were to guide the final selection of the inverter.

TABLE 3-7

SPECIFICATIONS OF THE CEA2-C-130Z-252 INVERTER

Output Voltage:	130 VDC nominal, adjustable from 123 to 137
Output Current:	2.5 A
Input Voltage	28 VDC nominal, 21-30 VDC acceptable
Efficiency:	80% maximum
Regulation:	Line – 1% , 21-30 V input change Load – 1% , .25-2.5 A load change
Ripple:	1% pp
Temperature Coefficient:	.05%/ ^{o}C
Size:	7 1/16 x 7 1/16 x 5 9/16 in.^{3}
Weight:	10 1 b
Cost:	$525 , 1 - 4 units

4.0 HARDWARE DELIVERIES

Two types of hardware delivery are required by the present contract. First, a breadboard transmitter, whose specifications and development have been described in earlier sections of this report, is to be delivered at the conclusion of the technical effort. Second, six high-power, high-efficiency GaAs Read IMPATT diodes representative of those to be used in the transmitter are to be delivered at the end of each month of the technical effort.

The first six diode deliveries were completed by 30 September 1976. The first three of these consisted of four-mesa diodes of the type originally proposed for use in the transmitter output stage. Mesa diameters were typically 7-8 mils. The next three shipments contained diodes with four 10-mil-diameter mesas. These larger diodes are to be used in the deliverable transmitter.

Condensed performance data for all diodes delivered are given in Table 4-1. These data were obtained in CW oscillator tests of the diodes in a disc-resonator-in-waveguide or "top-hat" circuit. More detailed data were supplied with the diode shipments.

Six additional diode deliveries are to be made during the remainder of the program.

TABLE 4-1

PERFORMANCE DATA AT MAXIMUM CW POWER OUTPUT
FOR DIODES DELIVERED DURING THE FIRST HALF OF THE PROGRAM

Diode	V(Volts)	I(mA)	P_o(W)	f(GHz)	η(%)	T_J^*(^oC)
Lot 1						
768-1	100.6	460	11.25	4.909	24.3	219
768-3	97.8	460	10.58	5.291	23.5	212
768-6	99.5	440	10.73	5.155	24.5	218
768-10	105.8	440	10.93	4.775	23.5	225
777-6	96.0	480	10.44	4.880	22.7	229
777-8	100.9	480	11.45	4.806	23.6	210
Lot 2						
756B-6	101.1	460	10.57	4.896	22.7	223
756B-8	99.8	470	10.13	4.838	21.6	220
756D-3	99.9	450	10.17	5.110	22.6	214
756D-8	100.7	460	10.03	5.078	21.7	236
768A-2	105.9	460	10.46	4.947	21.5	277
777-1	94.4	500	10.71	4.854	22.7	226
Lot 3						
756B-1	101.6	480	11.05	4.892	22.7	202
756E-3	97.0	500	10.14	5.010	20.9	255
756F-4	99.2	480	10.58	4.948	22.2	236
768B-1	98.5	450	10.16	5.141	22.9	262
777A-9	97.5	500	11.62	4.865	23.8	218
777A-10	98.3	480	11.40	4.860	24.2	230

*40° C Heat Sink Assumed.

TABLE 4-1 (Cont'd)

PERFORMANCE DATA AT MAXIMUM CW POWER OUTPUT
FOR DIODES DELIVERED DURING THE FIRST HALF OF THE PROGRAM

Diode	V(Volts)	I(mA)	P_o(W)	f(GHz)	η(%)	T_J^*(^oC)
Lot 4						
904D-4	64.4	820	12.50	6.630	23.7	-
904D-8	66.4	800	13.16	6.662	24.8	-
904F-1	68.8	800	12.77	6.512	23.2	222
904F-2	65.2	820	12.83	6.661	24.0	207
904G-2	63.2	840	12.50	6.629	23.6	198
904G-5	62.7	860	12.61	6.623	23.4	193
Lot 5						
907A-3	83.5	782	16.22	5.332	24.9	-
907A-4	87.4	744	15.32	5.319	23.6	-
907A-11	86.6	744	14.70	5.194	22.8	-
910-5	114.0	532	17.39	4.842	28.7	223
910-16	113.4	500	16.80	4.885	29.6	196
910A-5	114.2	560	17.02	4.855	26.6	216
Lot 6						
907B-8	88.3	782	17.17	5.210	24.9	-
907B-15	86.2	782	16.75	5.220	24.9	-
909-2	104.7	650	19.28	4.873	28.3	229
909-3	107.0	669	20.10	4.830	28.1	225
910A-6	108.5	560	15.57	4.813	25.6	215
910C-9	114.1	560	17.06	4.831	26.7	-

*40^oC Heat Sink Assumed.

5.0 PROGRAM STATUS AND PLANS

The purpose of this section is to summarize the status of the program as of 29 September 1976, and to outline the tasks to be addressed during the remainder of the program period. Details of the work accomplished have been presented in the foregoing sections.

5.1 Program Status

The transmitter system design has been completed. Four major subassemblies make up the deliverable breadboard transmitter. These are the VCO-driver, the multiple-diode power output stage, the multichannel current regulator feeding the output stage, and the DC-to-DC inverter supplying high voltage to all IMPATT diodes in the transmitter. The transmitter operates from a 28-VDC primary power source, and uses GaAs Read IMPATT diodes for RF power generation.

Design, fabrication, and testing of the VCO-driver subassembly have been completed. This unit is awaiting integration with the remaining parts of the transmitter, after which testing of the complete system will be undertaken.

The transmitter output stage development is the major program task. Epitaxial material growth and diode fabrication procedures which repeatably produce GaAs Read IMPATT diodes with more than 15-W CW output and 25 percent DC-to-RF conversion efficiency have been demonstrated.

Four 15-W diodes are to be used in the output stage. Monthly shipments, each containing six diodes representative of those to be used in the output stage, have been made to RADC. The general form of the output stage circuit has been selected. A nonresonant parallel-type power combiner using a multiport hybrid of the type described by Gysel[5] has been chosen. Analysis has shown that this type of circuit can meet the conditions for isolation and low loss required in the output stage. To this will be coupled four individual oscillator modules.

Preliminary RF circuit design for the oscillator modules has been completed. Both the power combiner and the oscillator modules are to be realized in trapped inverted microstrip (TIM) line. Components for some basic TIM-line structures and for a two-port Gysel hybrid have been fabricated and are awaiting test. A backup output stage design using a dielectrically loaded resonant-cavity power combiner similar to the circuit developed during the previous program[2] has been prepared for use if difficulties are encountered with the previously untried TIM-line circuits.

Circuit design for the multichannel current regulator is complete. Fabrication, test, and possible refinement remain to be accomplished.

A standard, commercially available DC-to-DC inverter is to be used in the transmitter. One suitable unit has been selected and, based on the use of this unit, projections of overall transmitter power consumption have been made.

5.2 Plans

No further development work should be required on the VCO-driver. We must still integrate it with the transmitter package and perform final testing.

Several tasks remain in the output stage development. Additional epitaxial material must be grown so that more diodes can be fabricated. The diodes will form an inventory for use in meeting future delivery requirements and for use in output stage development. The basic TIM-line circuit components now on hand must be assembled and tested. Following successful tests of these circuits, final design, assembly, and test of the four-port power combiner can be undertaken. Measurements of diode terminal impedance must be made to complete the RF design of the oscillator modules. Bias circuit design, mechanical design, fabrication, assembly, and test will then follow. The resonant-cavity power-combiner design is being held for use in the output stage if necessary.

Using the existing design, the multichannel current regulator will be assembled and tested. It will then be integrated with the other transmitter components.

The DC-to-DC inverter is to be ordered. The possibility of reducing the size and weight and increasing the efficiency of existing designs is to be investigated through consultation with the inverter manufacturer.

When all transmitter components are on hand, they will be assembled into the deliverable transmitter package. Final performance testing will then take place.

Several analytical tasks must also be completed in the remainder of the program. Reliability data on the components in the transmitter must be reviewed to confirm that the operating life and shelf life requirements can indeed be met. A complete analysis of cost and possible cost-size-weight-performance tradeoffs must also be made. The deliverable transmitter will obviously not represent the highest level of design refinement possible. Prospects for future improvement in performance will be surveyed.

6.0 REFERENCES

1. C. A. Brackett, "The Elimination of Tuning-Induced Burnout and Bias Circuit Oscillations in IMPATT Oscillators," Bell System Technical J. 52, 271 (March 1973).

2. "High-Efficiency Solid-State C-Band Generator," Contract F30602-74-C-0306, work carried out at Raytheon Research Division from 24 June 1974 to 24 June 1975.

3. "High-Efficiency Solid-State C-Band Generator," Final Technical Report RADC-TR-75-286, Rome Air Development Center, Air Force Systems Command, Griffiss Air Force Base, New York 13441, November 1975.

4. E. J. Wilkinson, "An N-Way Hybrid Power Divider," IRE Transactions MTT-8, 116 (January 1960).

5. U. H. Gysel, "A New N-Way Power Divider/Combiner Suitable for High-Power Applications," 1975 IEEE MTT Symposium Digest, p. 116.

6. C. Buntschuh, "A Study of the Transmission Line Properties of Trapped Inverted Microstrip Line," Final Technical Report RADC-TR-74-311, Rome Air Development Center, Air Force Systems Command, Griffiss Air Force Base, New York 13441, December 1974.

7. D. J. Coleman, Jr., W. R. Wisseman, and D. W. Shaw, "Reaction Rates for Pt on GaAs," Appl. Phys. Lett. 24, 355 (April 1974).

AD-A044 034 RAYTHEON CO WALTHAM MASS RESEARCH DIV F/G 9/5
COST-EFFECTIVE GAAS READ IMPACT TRANSMITTERS.(U)
MAY 77 R N WALLACE F30602-76-0143
UNCLASSIFIED S-2166 RADC-TR-77-178 NL

2 OF 2
AD
A044034

END
DATE
FILMED
10-77
DDC

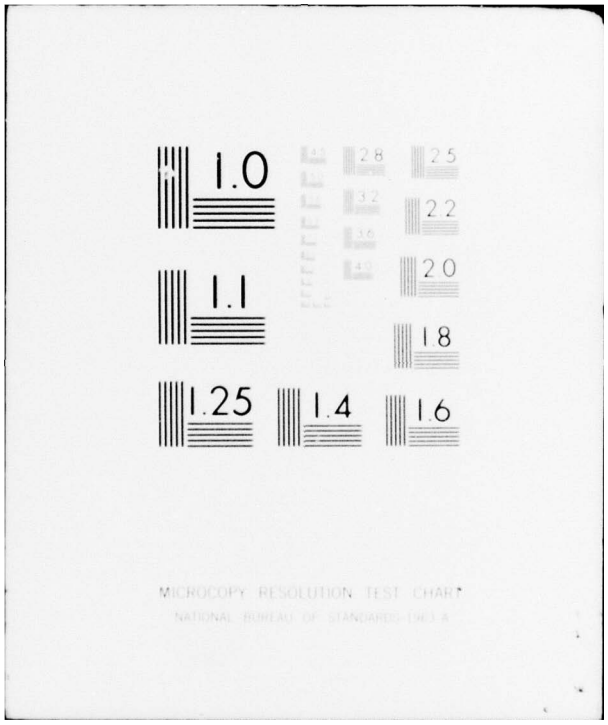
1.0
1.1
1.25
1.4
1.6
2.8
2.5
3.2
2.2
3.6
2.0
4.0
1.8
MICROCOPY RESOLUTION TEST CHART
NATIONAL BUREAU OF STANDARDS 1963 A

METRIC SYSTEM

BASE UNITS:

Quantity	Unit	SI Symbol	Formula
length	metre	m	...
mass	kilogram	kg	...
time	second	s	...
electric current	ampere	A	...
thermodynamic temperature	kelvin	K	...
amount of substance	mole	mol	...
luminous intensity	candela	cd	...

SUPPLEMENTARY UNITS:

plane angle	radian	rad	...
solid angle	steradian	sr	...

DERIVED UNITS:

Acceleration	metre per second squared	...	m/s
activity (of a radioactive source)	disintegration per second	...	(disintegration)/s
angular acceleration	radian per second squared	...	rad/s
angular velocity	radian per second	...	rad/s
area	square metre	...	m
density	kilogram per cubic metre	...	kg/m
electric capacitance	farad	F	A·s/V
electrical conductance	siemens	S	A/V
electric field strength	volt per metre	...	V/m
electric inductance	henry	H	V·s/A
electric potential difference	volt	V	W/A
electric resistance	ohm		V/A
electromotive force	volt	V	W/A
energy	joule	J	N·m
entropy	joule per kelvin	...	J/K
force	newton	N	kg·m/s
frequency	hertz	Hz	(cycle)/s
illuminance	lux	lx	lm/m
luminance	candela per square metre	...	cd/m
luminous flux	lumen	lm	cd·sr
magnetic field strength	ampere per metre	...	A/m
magnetic flux	weber	Wb	V·s
magnetic flux density	tesla	T	Wb/m
magnetomotive force	ampere	A	...
power	watt	W	J/s
pressure	pascal	Pa	N/m
quantity of electricity	coulomb	C	A·s
quantity of heat	joule	J	N·m
radiant intensity	watt per steradian	...	W/sr
specific heat	joule per kilogram-kelvin	...	J/kg·K
stress	pascal	Pa	N/m
thermal conductivity	watt per metre-kelvin	...	W/m·K
velocity	metre per second	...	m/s
viscosity, dynamic	pascal-second	...	Pa·s
viscosity, kinematic	square metre per second	...	m/s
voltage	volt	V	W/A
volume	cubic metre	...	m
wavenumber	reciprocal metre	...	(wave)/m
work	joule	J	N·m

SI PREFIXES:

Multiplication Factors	Prefix	SI Symbol
1 000 000 000 000 = 10^{12}	tera	T
1 000 000 000 = 10^{9}	giga	G
1 000 000 = 10^{6}	mega	M
1 000 = 10^{3}	kilo	k
100 = 10^{2}	hecto*	h
10 = 10^{1}	deka*	da
0.1 = 10^{-1}	deci*	d
0.01 = 10^{-2}	centi*	c
0.001 = 10^{-3}	milli	m
0.000 001 = 10^{-6}	micro	μ
0.000 000 001 = 10^{-9}	nano	n
0.000 000 000 001 = 10^{-12}	pico	p
0.000 000 000 000 001 = 10^{-15}	femto	f
0.000 000 000 000 000 001 = 10^{-18}	atto	a

* To be avoided where possible.

MISSION
of
Rome Air Development Center

RADC plans and conducts research, exploratory and advanced development programs in command, control, and communications (C^3) activities, and in the C^3 areas of information sciences and intelligence. The principal technical mission areas are communications, electromagnetic guidance and control, surveillance of ground and aerospace objects, intelligence data collection and handling, information system technology, ionospheric propagation, solid state sciences, microwave physics and electronic reliability, maintainability and compatibility.

Printed by
United States Air Force
Hanscom AFB, Mass. 01731